

Decoherence of Josephson coupling and thermal quenching of the Josephson diode effect in bilayer superconductors

F. Yang,^{1,*} C. Y. Dong,¹ Joshua A. Robinson,¹ and L. Q. Chen^{1,†}

¹*Department of Materials Science and Engineering and Materials Research Institute, The Pennsylvania State University, University Park, PA 16802, USA*

(Dated: February 20, 2026)

Motivated by recent studies on superconducting (SC) diode nonreciprocity, we uncover an unexpected hierarchy of SC-phase decoherence in bilayer superconductors hosting both interlayer Josephson coupling and a Josephson diode effect. Contrary to the conventional single-energy-scale paradigm where Josephson coherence and diode nonreciprocity vanish simultaneously at the SC gap-closing temperature, we demonstrate, using a self-consistent microscopic theory incorporating phase fluctuations, that the system undergoes a sequence of distinct thermal crossovers upon heating: the diode effect disappears first at T_η , Josephson coherence is subsequently lost at T_c , and the SC gap collapses only at a higher temperature T_s . Rather than a direct SC-normal transition, the system thus evolves through successive nonreciprocal, reciprocal, and incoherent Josephson regimes before entering the normal state. Counterintuitively, the separation between these regimes is governed not only by interlayer coupling, but also sensitively by in-plane disorder and carrier density. These findings point to a generic hierarchy of SC decoherence in low-dimensional Josephson systems, and suggest broader relevance to layered superconductors, including cuprates and recently discovered nickelates, as well as to SC qubits.

Introduction.—Over the past few decades, Josephson junctions, where two superconductors are coupled through a non-superconducting barrier [1], have emerged not only as the basis of a wide range of superconducting (SC) electronic devices [2–4], but also as essential building blocks of quantum technologies and quantum computation [5–7]. In conventional Josephson junctions with a classical or centrosymmetric barrier, SC transport is reciprocal. This reciprocity originates from the current–phase relation (CPR) of the Josephson supercurrent I_J as a function of the SC phase difference ϕ between the two electrodes [8], which takes the generalized form $I_J(\phi) = |J_1||\Delta_1||\Delta_2| \sin(\phi) + 2|J_2||\Delta_1|^2|\Delta_2|^2 \sin(2\phi)$. Here, $|J_1|$ and $|J_2|$ denote the amplitudes of the first and second harmonics, respectively, and $|\Delta_1|$ and $|\Delta_2|$ are the SC gaps of the two electrodes. Because of this CPR, the critical supercurrent is identical for opposite current directions, reflecting the reciprocal nature of conventional Josephson transport.

Recently, by analogy with p – n junctions in semiconductor technology which permit low-resistance charge transport in one direction but high resistance in the opposite one, the realization of a Josephson diode effect, i.e., a non-reciprocal critical supercurrent, has attracted considerable attention [9–19]. Such an effect enables directional control of dissipationless supercurrents and is of both fundamental interest and practical importance for applications in SC electronics. Realizing the SC diode effect requires the breaking of time-reversal symmetry (and often inversion symmetry) [20], which results in a generalized asymmetric CPR [14, 21, 22],

$$I_J(\phi) = |J_1||\Delta_1||\Delta_2| \sin(\phi + \alpha) + 2|J_2||\Delta_1|^2|\Delta_2|^2 \sin(2\phi), \quad (1)$$

where $\alpha \neq 0$ signals the absence of time-reversal symmetry. As a result, as shown in Fig. 1(b), the maximum supercurrent flowing in the positive direction differs from that in the negative direction, giving rise to non-reciprocal critical currents and the Josephson diode behavior, as experimentally observed in Josephson junction systems with time-reversal symmetry

breaking [14]. In particular, with the rapid development of advanced quantum materials, the Josephson diode behavior has been experimentally and theoretically explored in low-dimensional junctions, including a variety of multilayer and bilayer platforms [18, 22–30]. Such Josephson junctions can host engineered asymmetry, for example arising from twist angles [22, 23, 25–29], offering a versatile and highly tunable route toward controlling the Josephson diode behavior.

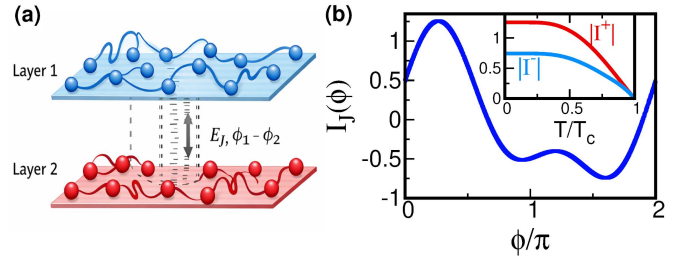


FIG. 1. (a) Schematic illustration of a bilayer superconductor with interlayer Josephson coupling. (b) The CPR given by Eq. (1). Inset: Temperature dependence of the critical-current strength (normalized) in the forward and backward directions from Eq. (1) based on the mean-field BCS theory to calculate the SC gap. For simplicity and without loss of generality, we set $\alpha = 0.2\pi$ and $|J_1| = 4|J_2||\Delta_1||\Delta_2|$.

Within the conventional CPR paradigm of Josephson junctions and Josephson diodes [Eq. (1)], both Josephson coherence and diode non-reciprocity, are expected to disappear simultaneously at the characteristic temperature where the SC gap vanishes. In this work, however, we emphasize the central role of SC phase coherence and rigorously demonstrate, within a self-consistent microscopic framework incorporating SC phase fluctuations, that low-dimensional Josephson junctions, such as bilayer superconductors, undergo a sequence of distinct thermal crossovers upon heating (summarized in Fig. 3(a)). Specifically, as temperature increases, the system evolves from a non-reciprocal Josephson phase to a reciprocal

phase, followed by an incoherent Josephson state, and finally into the normal state, such that the Josephson diode effect disappears first at a characteristic temperature T_η , followed by the loss of Josephson coherence at T_c , and finally the vanishing of the SC gap at a higher temperature T_s . These findings reveal a hierarchy of decoherence processes that are generic to low-dimensional Josephson systems and, more broadly, can potentially be extended to understand layered SC materials, such as cuprates [31–38] and recently discovered nickelates [39–44], particularly their c -axis transport behaviors.

Model.—We start with a minimal mean-field Hamiltonian description [45, 46] of a bilayer superconductor with interlayer Josephson coupling, as schematically illustrated in Fig. 1(a),

$$H = \sum_{j=1,2} \left[\int d\mathbf{x} \Psi_j^\dagger(\mathbf{x}) \begin{pmatrix} \xi_{j\hat{\mathbf{p}}} & \Delta_j(\mathbf{x}) \\ \Delta_j^*(\mathbf{x}) & \xi_{j\hat{\mathbf{p}}} \end{pmatrix} \Psi_j(\mathbf{x}) - \frac{|\Delta_j|^2}{U} \right] - \frac{1}{2} (J_1 \Delta_1 \Delta_2^* + c.c.) - \frac{1}{2} [J_2 (\Delta_1 \Delta_2^*)^2 + c.c.] + H_I, \quad (2)$$

where $\Psi_j^\dagger = (c_{j\uparrow}^\dagger, c_{j\downarrow}^\dagger)$ is the Nambu spinor in layer j with $c_{j\uparrow}^\dagger$ and $c_{j\downarrow}^\dagger$ being the creation and annihilation operators, respectively; $\xi_{j\mathbf{k}}$ denotes the single-particle dispersion measured from the chemical potential, and $U < 0$ is the SC pairing interaction; the momentum operator $\hat{\mathbf{p}} = -i\hbar\nabla$, while \mathbf{x} denotes the spatial coordinate confined to the in-plane space of each layer; H_I denotes the long-range Coulomb interactions (Sec. SI). The SC order parameter in each layer reads [45, 46]

$$\Delta_j(\mathbf{x}) = |\Delta_j| e^{i\phi_j(\mathbf{x})}, \quad (3)$$

where $|\Delta_j|$ and $\phi_j(\mathbf{x})$ are the SC gap and phase, respectively. Here the interlayer Josephson coupling includes both the conventional first harmonic and a higher-order second harmonic contribution, and $J_{1,2}$ are generally complex interlayer Josephson amplitudes [14, 21, 22]. Within the conventional derivation of the Josephson effect [47, 48], these couplings originate from the interlayer hopping of electrons, which mediates the tunneling of Cooper pairs between the two SC layers. While the first harmonic J_1 arises from the lowest-order tunneling of a single Cooper pair, the second harmonic J_2 emerges from higher-order tunneling processes, involving correlated tunneling of two Cooper pairs via virtual intermediate states [47].

We consider the symmetric bilayer case and assume identical electronic structures in the two layers, i.e., $\xi_{j\mathbf{k}} = \xi_{\mathbf{k}}$, thereby yielding $|\Delta_j| = |\Delta|$. In addition, we consider a complex first-harmonic Josephson coupling $J_1 = |J_1| e^{i\alpha}$, while the second-harmonic coupling is taken to be real, $J_2 = J_2^*$. The phase shift α represents a nontrivial relative phase between different Josephson harmonics that explicitly breaks time-reversal symmetry, such that $2\arg(J_1) \neq \arg(J_2)$, and cannot be removed by a global redefinition of the Josephson phases. Such a phase shift can arise from the interplay of interlayer twist effect [11, 13, 20–23, 25–29], which generates multiple inequivalent tunneling channels, and external or internally generated effective magnetic fields that imprint phase frustration onto these channels. The present work further explores the physical implications of the SC phase coherence.

To consider the SC phase coherence, we introduce the relative (Josephson) and total SC phase fields as

$$\phi(\mathbf{x}) = \phi_1(\mathbf{x}) - \phi_2(\mathbf{x}), \quad (4)$$

$$\theta(\mathbf{x}) = [\phi_1(\mathbf{x}) + \phi_2(\mathbf{x})]/2. \quad (5)$$

Within path-integral formalism, integrating out the fermionic degrees of freedom leads to an effective action (Sec. SI)

$$S_{\text{eff}} = S_{\text{intra}}(|\Delta|, \mathbf{p}_s^2) + S_J(\phi). \quad (6)$$

Here, S_{intra} governs the intralayer SC properties, while $\mathbf{p}_s = \nabla\theta(\mathbf{x})/2$ is the physically meaningful, gauge-invariant quantity describing fluctuations of the total phase $\theta(\mathbf{x})$ [49, 50]. These fluctuations correspond to the in-phase collective mode [50–52], associated with the bosonic Nambu–Goldstone (NG) mode of the SC state [53–56], and involve long-range Coulomb interactions in the symmetric channel. In 2D systems, this mode remains gapless and an active collective excitation [52, 57–60], in contrast to the dynamically inert case in 3D [61, 62], where the NG mode is fully gapped out by the Anderson–Higgs mechanism [63]. In our recent works for 2D superconductors [58–60], we have self-consistently incorporated these finite NG-phase fluctuations into the SC gap equation in the presence of long-range Coulomb interactions. As a result, the SC gap and its disappearance temperature T_s acquire nontrivial dependence on disorder and carrier density, reflecting fluctuation-induced renormalization effects beyond mean-field theory [58–60]. For completeness, we directly adopt this approach for the in-plane sector to determine $|\Delta(T)|$ and $\langle \mathbf{p}_s^2 \rangle$ (see Sec. SIII), which enter the subsequent interlayer Josephson formulation as external inputs. Nevertheless, the central result derived below follows from general physics and gauge-invariant considerations and does not depend on the specific microscopic realization of these quantities.

The essential effective action for the interlayer Josephson coupling and the out-of-phase collective mode (known as the Leggett-type [64] Josephson phase mode) reads

$$S_J(\phi) = \int dR \left\{ \frac{D_I}{2} \left(\frac{\partial_t \phi}{2} \right)^2 - \frac{f_s}{4} \left(\frac{\nabla \phi}{2} \right)^2 + |J_1| |\Delta|^2 \cos(\phi + \alpha) + |J_2| |\Delta|^4 \cos(2\phi) \right\}. \quad (7)$$

Here, D_I denotes the effective density of states renormalized by the interlayer long-range Coulomb interactions, and f_s is the phase stiffness, written as (see Sec. SI for detailed derivation)

$$f_s = f_s(|\Delta|^2, \langle \mathbf{p}_s^2 \rangle) = \frac{v_F^2 |\Delta|^2}{1 + \xi/l} \sum_{\mathbf{k}} \frac{f(E_{\mathbf{k}}^-) - f(E_{\mathbf{k}}^+)}{2E_{\mathbf{k}}^3}, \quad (8)$$

which depends on gap $|\Delta(T)|$ and NG phase fluctuations $\langle \mathbf{p}_s^2 \rangle$. Here, the fermionic quasiparticle spectrum $E_{\mathbf{k}}^\pm = \mathbf{v}_{\mathbf{k}} \cdot \mathbf{p}_s \pm E_{\mathbf{k}}$ with $E_{\mathbf{k}} = \sqrt{\xi_{\mathbf{k}}^2 + |\Delta|^2}$; the prefactor $(1 + \xi/l)^{-1}$ accounts for the disorder-induced reduction of the phase stiffness, consistent with Tinkham’s interpolation [65] and subsequent microscopic studies [45, 66–68], where $\xi = \hbar v_F / |\Delta|$ is the SC coherence length and $l = v_F \tau$ is the mean free path with τ being

the effective scattering time. Within a parabolic-band approximation, f_s reduces to the familiar form n_s/m^* [50–52, 66, 68], with n_s being superfluid density and m^* the effective mass.

According to the action $S_J(\phi)$, the interlayer Josephson coupling explicitly gaps the out-of-phase mode. We show in the following that the Josephson decoherence proceeds through smooth renormalization. Specifically, we decompose the Josephson phase as $\phi = \phi_e + \delta\phi$ where $\delta\phi$ represents Josephson phase fluctuations around equilibrium configuration ϕ_e . With $\langle\delta\phi\rangle = 0$, using the cumulant expansion (see Sec. III. A for detailed derivations)

$$\langle\cos(n\phi)\rangle = \text{Re}[e^{in\phi_e}\langle e^{in\delta\phi}\rangle] = \cos(n\phi_e)e^{-n^2\langle\delta\phi^2\rangle/2}, \quad (9)$$

the thermally averaged Josephson energy reads

$$\begin{aligned} E_J(\phi_e) &= -|J_1||\Delta|^2\langle\cos(\phi + \alpha)\rangle - |J_2||\Delta|^4\langle\cos(2\phi)\rangle \\ &= -\bar{J}_1(T)\cos(\phi_e + \alpha) - \bar{J}_2(T)\cos(2\phi_e), \end{aligned} \quad (10)$$

where the effective Josephson couplings are renormalized by Josephson phase fluctuations as

$$\bar{J}_1(T) = |J_1||\Delta(T)|^2 \exp[-\langle\delta\phi^2(T)\rangle/2], \quad (11)$$

$$\bar{J}_2(T) = |J_2||\Delta(T)|^4 \exp[-2\langle\delta\phi^2(T)\rangle]. \quad (12)$$

The optimal equilibrium phase ϕ_e^{op} is determined by global minimizer of the fluctuation-renormalized Josephson energy

$$\phi_e^{\text{op}} = \arg \min_{\phi_e \in [0, 2\pi)} E_J(\phi_e). \quad (13)$$

The Josephson phase fluctuations can be derived within the quantum statistic mechanism based on the equation of motion of Josephson phase fluctuations $\delta\phi$ obtained from the action $S_J(\phi)$ (Sec. II. B), and their average is derived as (Sec. III. C)

$$\langle\delta\phi^2(T)\rangle = \int \frac{2d\mathbf{q}}{(2\pi)^2} \frac{2n_B[\omega_L(q)] + 1}{D_I\omega_L(q)}, \quad (14)$$

which corresponds to the standard bosonic excitation, consisting of contributions from both thermal excitations $2n_B(\omega_L)$ (thermal fluctuations) and zero-point oscillations (quantum fluctuations). Here, the function $n_B(x)$ is the Bose distribution. The excitation spectrum $\omega_L(q)$ of this Leggett-type [64] collective phase mode is determined by

$$D_I\omega_L^2(q) = 4\bar{J}_1\cos(\phi_e^{\text{op}} + \alpha) + 16\bar{J}_2\cos(2\phi_e^{\text{op}}) + f_s q^2/2, \quad (15)$$

corresponding to a massive (gapped) collective excitation.

Consequently, Eqs. (10)–(15) form a nontrivial closed set of self-consistent equations, which determine the effective Josephson couplings $\bar{J}_1(T)$ and $\bar{J}_2(T)$ renormalized by the Josephson phase fluctuations. Further considering the Josephson supercurrent injection I_J (Sec. III. A), this procedure yields a qualitatively modified Josephson CPR,

$$I_J(\phi_e) = 2e[\bar{J}_1(T)\sin(\phi_e + \alpha) + 2\bar{J}_2(T)\sin(2\phi_e)]. \quad (16)$$

Consequently, the Debye–Waller–like factors [69, 70] appearing in the Josephson couplings, $\exp(-\langle\delta\phi^2(T)\rangle/2)$ in $\bar{J}_1(T)$

and $\exp(-2\langle\delta\phi^2(T)\rangle)$ in $\bar{J}_2(T)$, which originate from Josephson phase fluctuations, render the temperature dependence of the Josephson CPR no longer governed solely by a single energy scale set by the SC gap as in Eq. (1). These factors, in fact, encode the decoherence of the Josephson coupling induced by SC phase fluctuations, yielding a Josephson response that is governed by both the SC gap and Josephson phase coherence.

In particularly, in the limit where $\bar{J}_1 \rightarrow 0$ and $\bar{J}_2 \rightarrow 0$ as a consequence of significant Josephson phase fluctuations, while the SC gap $|\Delta|$ remains finite, the equilibrium Josephson phase can no longer be uniquely determined from the minimum of the Josephson energy E_J in Eq. (10). This indicates that SC phase coherence across the Josephson junction is not established, despite the presence of a finite pairing gap.

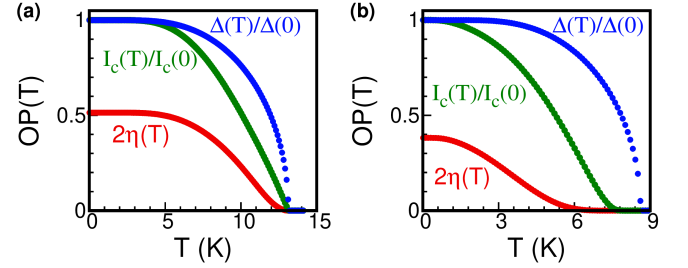


FIG. 2. Temperature dependence of the Josephson critical current, the diode efficiency and the SC gap self-consistently calculated by (a) mean-field and (b) phase-fluctuation theories. We set $\tau|\Delta_{\text{MF}}(0)| = 0.2$, $v_F = 10^5$ m/s and $|\Delta_{\text{MF}}(0)| = 2$ meV, where $|\Delta_{\text{MF}}(0)|$ is the zero-temperature gap from mean-field theory.

Results.—We perform fully self-consistent numerical calculations, incorporating both the intralayer SC properties $|\Delta(T)|$ and $\langle p_s^2(T) \rangle$, and the proposed Josephson-related framework in this study [Eqs. (10)–(15)]. The specific model parameters used in simulation are provided in the Supplemental Material (Sec. SIV). Following previous works [14, 21, 22], we define the Josephson critical current as $I_c(T) = \max(|I_c^+(T)|, |I_c^-(T)|)$, and introduce the diode efficiency

$$\eta(T) = \left| \frac{|I_c^+(T)| - |I_c^-(T)|}{|I_c^+(T=0)| + |I_c^-(T=0)|} \right| \quad (17)$$

which quantifies the relative strength of the nonreciprocal Josephson response at finite temperatures, normalized to its $T = 0$ value. Here, $I_c^+(T)$ and $I_c^-(T)$ denote the critical Josephson currents for positive and negative current directions, respectively. For comparison, results obtained with and without phase fluctuations are shown in Fig. 2. It is noted that even at $T = 0$, including the contribution from the zero-point Josephson phase fluctuations suppresses the zero-temperature diode efficiency $\eta(0)$, while the NG and Josephson phase fluctuations also reduce the zero-temperature gap $|\Delta(0)|$ (as discussed in Refs. [58–60]) and the critical current $I_c(0)$ (see Sec. SV for more details related to zero-point oscillations), respectively. This zero-point effect suggests the intrinsic quantum sensitivity of low-dimensional Josephson-diode systems,

and it represents a fundamental quantum limitation that cannot be circumvented by cooling. Quantum fluctuations therefore impose an intrinsic limit on Josephson coherence and nonreciprocal transport in low-dimensional Josephson systems.

For the essential critical behaviors, in the absence of phase fluctuations, as shown in Fig. 2(a), both SC and Josephson properties are solely determined by the SC gap, such that the Josephson critical current $I_c(T)$ and the diode efficiency $\eta(T)$ vanish at the same temperature at which the SC gap $|\Delta(T)|$ closes. In contrast, when significant Josephson phase fluctuations are activated, as shown in Fig. 2(b), a clear separation of energy scales emerges upon increasing temperature: the diode efficiency $\eta(T)$ disappears first, followed by the suppression of the Josephson critical current $I_c(T)$, while the SC gap $|\Delta(T)|$ remains finite and vanishes only at a higher temperature.

This is because that when Josephson phase fluctuations are activated, the Debye–Waller–like factors in \bar{J}_1 and \bar{J}_2 lead to a rapid suppression of the effective Josephson couplings as the fluctuation strength increases with temperature. As a result, the Josephson coupling is exponentially reduced by Josephson phase fluctuations, even in a regime where the SC gap remains finite, causing the Josephson effect to vanish at a temperature T_c lower than the gap-closing temperature T_s . Importantly, higher-order Josephson couplings are suppressed more strongly than the lowest-order term: the second-harmonic coupling $\bar{J}_2 \propto \exp(-2\langle\delta\phi^2\rangle)$ decays parametrically faster than the first-harmonic coupling $\bar{J}_1 \propto \exp(-\langle\delta\phi^2\rangle/2)$ as phase fluctuations increase with temperature. This hierarchy implies that non-sinusoidal components of the Josephson current–phase relation are particularly fragile against phase decoherence, with higher-order harmonics (e.g., $n \geq 3$) expected to be even more fragile according to Eq. (9). Since the Josephson diode nonreciprocity heavily relies on these non-sinusoidal components [14, 21, 22], the Josephson diode effect is expected to disappear at a temperature T_η lower than the critical temperature T_c at which the Josephson critical current is suppressed.

The emergence of three distinct temperature scales suggests the crucial role of Josephson-phase coherence in stabilizing nonreciprocal Josephson transport in low-dimensional SC systems, allowing Josephson phenomena to disappear while the SC gap remains finite. Accordingly, as schematically summarized in Fig. 3(a), the system undergoes a sequence of distinct thermal crossovers upon heating: it first evolves from a nonreciprocal Josephson phase to a reciprocal Josephson phase at a characteristic temperature T_η , followed by an incoherent Josephson state at T_c , above which phase coherence across the Josephson junction is lost while the SC gap remains finite, and finally enters the normal state at T_s .

We emphasize that the renormalized Josephson couplings in Eqs. (11) and (12) are derived in a mathematically rigorous manner, without reliance on model-specific parameters or physical assumptions, and are therefore generic. Then, the key point is whether Josephson phase fluctuations can be effectively excited. Typically, the Josephson coupling is weak, such that the gap of the Josephson phase mode [$\omega_L(q=0)$ in Eq. (15)] lies below the SC gap, rendering it a thermally active

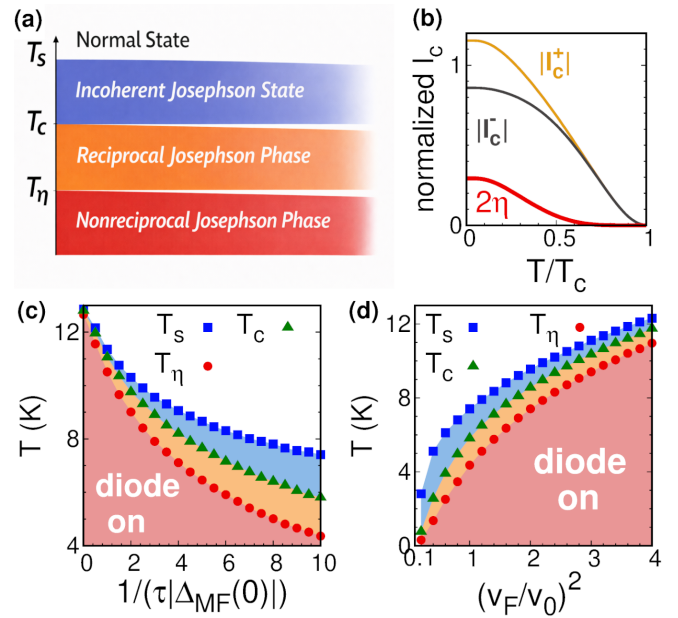


FIG. 3. (a) Schematic illustration of phase diagram upon heating. (b) Temperature dependence of the critical-current strength in the forward and backward directions. The distinct temperatures T_η , T_c , and T_s under reducing phase stiffness by (c) increasing disorder at $v_F = v_0$ and (d) reducing the Fermi velocity at $\tau|\Delta_{\text{MF}}(0)| = 0.1$. Here, $v_0 = 10^5$ m/s and $|\Delta_{\text{MF}}(0)| = 2$ meV, where $|\Delta_{\text{MF}}(0)|$ is the zero-temperature gap calculated from mean-field theory.

low-energy excitation. Notably, an equally important factor is the phase stiffness f_s , which determines the available phase space for bosonic phase fluctuations entering the fluctuation integrals [Eq. (14)]. In bulk systems, the phase stiffness is generally large, strongly suppressing phase fluctuations. By contrast, in low-dimensional systems the phase stiffness is significantly reduced, owing both to a smaller Fermi velocity and to the intrinsically enhanced disorder associated with reduced dimensionality [71, 72]. Increasing disorder and reducing the Fermi velocity, as shown in Figs. 3(c) and (d), respectively, lead to a suppression of T_s , T_c , T_η , while markedly increasing the separation among these characteristic temperatures. As a result, the hierarchy of SC decoherence scales becomes increasingly pronounced. Among these effects, the suppression of gap closing temperature T_s originates from the enhanced NG phase fluctuations (as discussed in Refs. [58–60]), whereas all the remaining Josephson features are primarily driven by the enhanced Josephson phase fluctuations (i.e., decoherence).

Discussion.—Beyond the conventional single-energy-scale paradigm of the Josephson CPR, the present study demonstrates that phase decoherence constitutes an independent and more fragile energy scale in low-dimensional Josephson systems, and hence, Josephson physics itself in this case splits into multiple decoherence regimes, including diode nonreciprocity as the most fragile scale. We therefore predict that the forward and backward critical currents in low-dimensional Josephson-diode systems, $|I_c^+(T)|$ and $|I_c^-(T)|$, to merge as

temperature increases, before vanishing altogether at T_c , as shown in Fig. 3(b). A similar tendency appears to be present in a wide range of recent experiments (e.g., Refs. [18, 19]), where the data exhibit a temperature evolution qualitatively consistent with that shown in Fig. 3(b).

It should be emphasized that the vanishing of the Josephson critical current and the disappearance of the diode effect correspond to exponential thermal crossovers, rather than conventional thermodynamic phase transitions of first or second order. Both the diode efficiency $\eta(T)$ and the Josephson critical current $I_c(T)$ shown in Fig 2(b) exhibit behaviors with continuous temperature derivatives in the vicinity of their respective disappearance temperatures, in contrast to the mean-field scenario shown in Fig 2(a), where discontinuities in temperature derivatives are expected. Consequently, these crossovers do not exhibit thermodynamic signatures such as latent heat or a jump in the specific heat, in contrast to the SC gap-closing transition, which is a genuine second-order phase transition [45, 46]. Such critical behaviors of the Josephson properties therefore constitute a key distinguishing feature between mean-field and fluctuation-based descriptions of Josephson systems.

The present work provides a tractable description of Josephson decoherence. Owing to the structural similarity [51, 60], this tractable framework can be naturally extended to layered superconductors with multilayer structures and Josephson coupling $J_c \cos(\theta_{n+1} - \theta_n)$ between different layers (where θ_n is the SC phase in the n -th layer), such as cuprates [31–38] and recently discovered nickelates [39–44], particularly for their c -axis transport behavior. In this context, one can anticipate the disappearance of c -axis superconductivity (zero-resistance) while the SC gap persists above a characteristic critical temperature. Moreover, owing to the close analogy in the underlying derivation of the excitations, similar considerations also apply to SC transmon qubits [73–75]. Our results indicate that higher-order Josephson harmonics are increasingly fragile against phase decoherence. This effect is expected to be relevant for the stability/coherence of Josephson-based SC qubits, where such higher harmonics play an essential role in determining the qubit spectrum and anharmonicity.

Acknowledgments.—This work is supported by the US Department of Energy, Office of Science, Basic Energy Sciences, under Award Number DE-SC0020145 as part of Computational Materials Sciences Program. F.Y. and L.Q.C. also appreciate the generous support from the Donald W. Hamer Foundation through a Hamer Professorship at Penn State.

* fzy5099@psu.edu

† lqc3@psu.edu

- [1] B. D. Josephson, The discovery of tunnelling supercurrents, *Rev. Mod. Phys.* **46**, 251 (1974).
- [2] M. Bal, C. Deng, J.-L. Orgiazzi, F. R. Ong, and A. Lupascu, Ultrasensitive magnetic field detection using a single artificial atom, *Nat. Commun.* **3**, 1324 (2012).
- [3] A. Wallraff, D. I. Schuster, A. Blais, L. Frunzio, R.-S. Huang, J. Majer, S. Kumar, S. M. Girvin, and R. J. Schoelkopf, Strong coupling of a single photon to a superconducting qubit using circuit quantum electrodynamics, *Nature* **431**, 162 (2004).
- [4] E. D. Walsh, W. Jung, G.-H. Lee, D. K. Efetov, B.-I. Wu, K.-F. Huang, T. A. Ohki, T. Taniguchi, K. Watanabe, P. Kim, D. Englund, and K. C. Fong, Josephson junction infrared single-photon detector, *Science* **372**, 409 (2021).
- [5] L. B. Ioffe, V. B. Geshkenbein, M. V. Feigel'man, A. L. Fauchère, and G. Blatter, Environmentally decoupled sds-wave josephson junctions for quantum computing, *Nature* **398**, 679 (1999).
- [6] J. Q. You, J. S. Tsai, and F. Nori, Scalable quantum computing with josephson charge qubits, *Phys. Rev. Lett.* **89**, 197902 (2002).
- [7] Y. Yu, S. Han, X. Chu, S.-I. Chu, and Z. Wang, Coherent temporal oscillations of macroscopic quantum states in a josephson junction, *Science* **296**, 889 (2002).
- [8] A. A. Golubov, M. Y. Kupriyanov, and E. Il'ichev, The current-phase relation in josephson junctions, *Rev. Mod. Phys.* **76**, 411 (2004).
- [9] A. Daido, Y. Ikeda, and Y. Yanase, Intrinsic superconducting diode effect, *Phys. Rev. Lett.* **128**, 037001 (2022).
- [10] S. Ilić and F. S. Bergeret, Theory of the supercurrent diode effect in rashba superconductors with arbitrary disorder, *Phys. Rev. Lett.* **128**, 177001 (2022).
- [11] N. F. Q. Yuan and L. Fu, Supercurrent diode effect and finite-momentum superconductors, *Proc. Natl. Acad. Sci. U.S.A.* **119**, e2119548119 (2022).
- [12] R. S. Souto, M. Leijnse, and C. Schrade, Josephson diode effect in supercurrent interferometers, *Phys. Rev. Lett.* **129**, 267702 (2022).
- [13] M. Davydova, S. Prembabu, and L. Fu, Universal josephson diode effect, *Sci. Adv.* **8**, eabo0309 (2022).
- [14] B. Pal, A. Chakraborty, P. K. Sivakumar, M. Davydova, A. K. Gopi, A. K. Pandeya, J. A. Krieger, Y. Zhang, M. Date, S. Ju, N. Yuan, N. B. M. Schröter, L. Fu, and S. S. P. Parkin, Josephson diode effect from cooper pair momentum in a topological semimetal, *Nat. Phys.* **18**, 1228 (2022).
- [15] F. Yang and L. Q. Chen, Altermagnetism-induced noncollinear superconducting diode effect and unidirectional superconducting transport, *Phys. Rev. B* **112**, L220502 (2025).
- [16] J. F. Steiner, L. Melischek, M. Trahms, K. J. Franke, and F. von Oppen, Diode effects in current-biased josephson junctions, *Phys. Rev. Lett.* **130**, 177002 (2023).
- [17] A. Kudriashov, X. Zhou, R. A. Hovhannisyan, A. S. Frolov, L. Elesin, Y. B. Wang, E. V. Zharkova, T. Taniguchi, K. Watanabe, Z. Liu, K. S. Novoselov, L. V. Yashina, X. Zhou, and D. A. Bandurin, Non-Majorana origin of anomalous current-phase relation and Josephson diode effect in $\text{Bi}_2\text{Se}_3/\text{NbSe}_2$ Josephson junctions, *Sci. Adv.* **11**, eadw6925 (2025).
- [18] Z. Wei, Y. Qiao, Y.-Y. Lyu, D. Wang, T. Li, L. R. Cadornim, P. Zhang, W.-C. Yue, D. Li, Z. Song, *et al.*, Scalable high-temperature superconducting diodes in intrinsic josephson junctions, arXiv:2508.06083 (2025).
- [19] M. S. Anwar, T. Nakamura, R. Ishiguro, S. Arif, J. W. A. Robinson, S. Yonezawa, M. Sigrist, and Y. Maeno, Spontaneous superconducting diode effect in non-magnetic Nb/Ru/Sr₂RuO₄ topological junctions, *Commun. Phys.* **6**, 290 (2023).
- [20] Y. Zhang, Y. Gu, P. Li, J. Hu, and K. Jiang, General theory of josephson diodes, *Phys. Rev. X* **12**, 041013 (2022).
- [21] P. A. Volkov, E. Lantagne-Hurtubise, T. Tummuru, S. Plugge, J. H. Pixley, and M. Franz, Josephson diode effects in twisted nodal superconductors, *Phys. Rev. B* **109**, 094518 (2024).
- [22] O. Can, T. Tummuru, R. P. Day, I. Elfimov, A. Damascelli, and

- M. Franz, High-temperature topological superconductivity in twisted double-layer copper oxides, *Nat. Phys.* **17**, 519 (2021).
- [23] S. Ghosh, V. Patil, A. Basu, Kuldeep, A. Dutta, D. A. Jangade, R. Kulkarni, A. Thamizhavel, J. F. Steiner, F. von Oppen, and M. M. Deshmukh, High-temperature josephson diode, *Nat. Mater.* **23**, 612 (2024).
- [24] H. Wu, Y. Wang, Y. Xu, P. K. Sivakumar, C. Pasco, U. Filippozzi, S. S. P. Parkin, Y.-J. Zeng, T. McQueen, and M. N. Ali, The field-free josephson diode in a van der waals heterostructure, *Nature* **604**, 653 (2022).
- [25] J.-X. Hu, Z.-T. Sun, Y.-M. Xie, and K. T. Law, Josephson diode effect induced by valley polarization in twisted bilayer graphene, *Phys. Rev. Lett.* **130**, 266003 (2023).
- [26] J. Díez-Mérida, A. Díez-Carlón, S. Y. Yang, Y.-M. Xie, X.-J. Gao, J. Senior, K. Watanabe, T. Taniguchi, X. Lu, A. P. Higginbotham, K. T. Law, and D. K. Efetov, Symmetry-broken josephson junctions and superconducting diodes in magic-angle twisted bilayer graphene, *Nat. Commun.* **14**, 2396 (2023).
- [27] A. Díez-Carlón, J. Díez-Mérida, P. Rout, D. Sedov, P. Virtanen, S. Banerjee, R. P. S. Penttilä, P. Altpeter, K. Watanabe, T. Taniguchi, S.-Y. Yang, K. T. Law, T. T. Heikkilä, P. Törmä, M. S. Scheurer, and D. K. Efetov, Probing the flat-band limit of the superconducting proximity effect in twisted bilayer graphene josephson junctions, *Phys. Rev. X* **15**, 041033 (2025).
- [28] S. Qi, J. Ge, C. Ji, Y. Ai, G. Ma, Z. Wang, Z. Cui, Y. Liu, Z. Wang, and J. Wang, High-temperature field-free superconducting diode effect in high- T_c cuprates, *Nat. Commun.* **16**, 531 (2025).
- [29] H. Wang, Y. Zhu, Z. Bai, Z. Lyu, J. Yang, L. Zhao, X. J. Zhou, Q.-K. Xue, and D. Zhang, Quantum superconducting diode effect with perfect efficiency above liquid-nitrogen temperature, *Nat. Phys.* **22**, 47 (2026).
- [30] H. Narita, J. Ishizuka, R. Kawarazaki, D. Kan, Y. Shiota, T. Moriyama, Y. Shimakawa, A. V. Ognev, A. S. Samardak, Y. Yanase, and T. Ono, Field-free superconducting diode effect in noncentrosymmetric superconductor/ferromagnet multilayers, *Nat. Nanotechnol.* **17**, 823 (2022).
- [31] E. Dagotto, Correlated electrons in high-temperature superconductors, *Rev. Mod. Phys.* **66**, 763 (1994).
- [32] T. Timusk and B. Statt, The pseudogap in high-temperature superconductors: an experimental survey, *Rep. Prog. Phys.* **62**, 61 (1999).
- [33] N. P. Armitage, P. Fournier, and R. L. Greene, Progress and perspectives on electron-doped cuprates, *Rev. Mod. Phys.* **82**, 2421 (2010).
- [34] J. C. S. Davis and D.-H. Lee, Concepts relating magnetic interactions, intertwined electronic orders, and strongly correlated superconductivity, *Proc. Natl. Acad. Sci.* **110**, 17623 (2013).
- [35] A. Damascelli, Z. Hussain, and Z.-X. Shen, Angle-resolved photoemission studies of the cuprate superconductors, *Rev. Mod. Phys.* **75**, 473 (2003).
- [36] B. Keimer, S. A. Kivelson, M. R. Norman, S. Uchida, and J. Zaanen, From quantum matter to high-temperature superconductivity in copper oxides, *Nature* **518**, 179 (2015).
- [37] J. G. Bednorz and K. A. Müller, Possible high T_c superconductivity in the Ba-La-Cu-O system, *Zeit. Phys. B* **64**, 189 (1986).
- [38] M.-K. Wu, J. R. Ashburn, C. Torng, P.-H. Hor, R. L. Meng, L. Gao, Z. J. Huang, Y. Wang, and A. Chu, Superconductivity at 93 K in a new mixed-phase Y-Ba-Cu-O compound system at ambient pressure, *Phys. Rev. Lett.* **58**, 908 (1987).
- [39] Y. Nomura and R. Arita, Superconductivity in infinite-layer nickelates, *Rep. Prog. Phys.* **85**, 052501 (2022).
- [40] B. Y. Wang, K. Lee, and B. H. Goodge, Experimental progress in superconducting nickelates, *Annu. Rev. Condens. Matter Phys.* **15**, 305 (2024).
- [41] D. Li, K. Lee, B. Y. Wang, M. Osada, S. Crossley, H. R. Lee, Y. Cui, Y. Hikita, and H. Y. Hwang, Superconductivity in an infinite-layer nickelate, *Nature* **572**, 624 (2019).
- [42] M. Xu, D. Qiu, M. Xu, Y. Guo, C. Shen, C. Yang, W. Sun, Y. Nie, Z.-X. Li, T. Xiang, L. Qiao, J. Xiong, and Y. Li, Anisotropic phase stiffness in infinite-layer nickelate superconductors, *Nat. Commun.* **16**, 6780 (2025).
- [43] M. Hepting, D. Li, C. J. Jia, H. Lu, E. Paris, Y. Tseng, X. Feng, M. Osada, E. Been, Y. Hikita, Y.-D. Chuang, Z. Hussain, K. J. Zhou, A. Nag, M. Garcia-Fernandez, M. Rossi, H. Y. Huang, D. J. Huang, Z. X. Shen, T. Schmitt, H. Y. Hwang, B. Moritz, J. Zaanen, T. P. Devereaux, and W. S. Lee, Electronic structure of the parent compound of superconducting infinite-layer nickelates, *Nat. Mater.* **19**, 381 (2020).
- [44] G.-M. Zhang, Y.-f. Yang, and F.-C. Zhang, Self-doped mott insulator for parent compounds of nickelate superconductors, *Phys. Rev. B* **101**, 020501 (2020).
- [45] A. A. Abrikosov, L. P. Gorkov, and I. E. Dzyaloshinski, *Methods of quantum field theory in statistical physics* (Courier Corporation, 2012).
- [46] J. Schrieffer, *Theory of Superconductivity* (W.A. Benjamin, 1964).
- [47] G. D. Mahan, *Many-particle physics* (Springer Science & Business Media, 2013).
- [48] G. Tkachov, Magnetoelectric andreev effect due to proximity-induced nonunitary triplet superconductivity in helical metals, *Phys. Rev. Lett.* **118**, 016802 (2017).
- [49] L. Benfatto, *The Berezinskii-Kosterlitz-Thouless Transition and its Application to Superconducting Systems* (2024).
- [50] F. Yang and M. W. Wu, Gauge-invariant microscopic kinetic theory of superconductivity: Application to the optical response of Nambu-Goldstone and Higgs modes, *Phys. Rev. B* **100**, 104513 (2019).
- [51] Z. Sun, M. M. Fogler, D. N. Basov, and A. J. Millis, Collective modes and terahertz near-field response of superconductors, *Phys. Rev. Res.* **2**, 023413 (2020).
- [52] F. Yang and M. W. Wu, Theory of coupled dual dynamics of macroscopic phase coherence and microscopic electronic fluids: Effect of dephasing on cuprate superconductivity, *Phys. Rev. B* **104**, 214510 (2021).
- [53] Y. Nambu, Nobel lecture: Spontaneous symmetry breaking in particle physics: A case of cross fertilization, *Rev. Mod. Phys.* **81**, 1015 (2009).
- [54] Y. Nambu, Quasi-particles and gauge invariance in the theory of superconductivity, *Phys. Rev.* **117**, 648 (1960).
- [55] J. Goldstone, Field theories with “superconductor” solutions, *II Nuovo Cimento* **19**, 154 (1961).
- [56] J. Goldstone, A. Salam, and S. Weinberg, Broken symmetries, *Phys. Rev.* **127**, 965 (1962).
- [57] S. Fischer, M. Hecker, M. Hoyer, and J. Schmalian, Short-distance breakdown of the Higgs mechanism and the robustness of the BCS theory for charged superconductors, *Phys. Rev. B* **97**, 054510 (2018).
- [58] F. Yang and L. Chen, A tractable framework for phase transitions in phase-fluctuating disordered 2D superconductors: applications to bilayer MoS₂ and disordered InO_x thin films, arXiv:2511.13268 (2025).
- [59] F. Yang, G. Zhao, Y. Shi, and L. Chen, An efficient phase-transition framework for gate-tunable superconductivity in monolayer WTe₂, arXiv:2509.08332 (2025).
- [60] F. Yang, Y. Shi, and L.-Q. Chen, Preformed cooper pairing and the uncondensed normal-state component in phase-fluctuating cuprate superconductivity, arXiv:2509.21133 (2025).

- [61] V. Ambegaokar and L. P. Kadanoff, Electromagnetic properties of superconductors, *Il Nuovo Cimento* **22**, 914 (1961).
- [62] P. B. Littlewood and C. M. Varma, Gauge-invariant theory of the dynamical interaction of charge density waves and superconductivity, *Phys. Rev. Lett.* **47**, 811 (1981).
- [63] P. W. Anderson, Plasmons, gauge invariance, and mass, *Phys. Rev.* **130**, 439 (1963).
- [64] A. J. Leggett, Number-phase fluctuations in two-band superconductors, *Prog. Theor. Phys.* **36**, 901 (1966).
- [65] M. Tinkham, *Introduction to superconductivity*, Vol. 1 (Courier Corporation, 2004).
- [66] F. Yang and M. W. Wu, Impurity scattering in superconductors revisited: Diagrammatic formulation of the supercurrent-supercurrent correlation and Higgs-mode damping, *Phys. Rev. B* **106**, 144509 (2022).
- [67] M. Silaev, Nonlinear electromagnetic response and Higgs-mode excitation in BCS superconductors with impurities, *Phys. Rev. B* **99**, 224511 (2019).
- [68] F. Yang and M. W. Wu, Gauge-invariant microscopic kinetic theory of superconductivity in response to electromagnetic fields, *Phys. Rev. B* **98**, 094507 (2018).
- [69] C. Kittel and C.-y. Fong, *Quantum theory of solids*, Vol. 5 (Wiley New York, 1963).
- [70] J. J. Sakurai and J. Napolitano, *Modern quantum mechanics* (Cambridge University Press, 2020).
- [71] Y. Saito, T. Nojima, and Y. Iwasa, Highly crystalline 2d superconductors, *Nat. Rev. Mater.* **2**, 16094 (2016).
- [72] D. Qiu, C. Gong, S. Wang, M. Zhang, C. Yang, X. Wang, and J. Xiong, Recent advances in 2d superconductors, *Adv. Mater.* **33**, 2006124 (2021).
- [73] S. M. Girvin *et al.*, Circuit qed: superconducting qubits coupled to microwave photons (2014).
- [74] J. Koch, T. M. Yu, J. Gambetta, A. A. Houck, D. I. Schuster, J. Majer, A. Blais, M. H. Devoret, S. M. Girvin, and R. J. Schoelkopf, Charge-insensitive qubit design derived from the cooper pair box, *Phys. Rev. A* **76**, 042319 (2007).
- [75] M. H. Devoret and R. J. Schoelkopf, Superconducting circuits for quantum information: An outlook, *Science* **339**, 1169 (2013).

Decoherence of Josephson coupling and thermal quenching of the Josephson diode effect in bilayer superconductors (Supplemental Materials)

F. Yang,^{1,*} C. Y. Dong,¹ Joshua A. Robinson,¹ and L. Q. Chen^{1,†}

¹*Department of Materials Science and Engineering and Materials Research Institute,
The Pennsylvania State University, University Park, PA 16802, USA*

SI. Derivation of the effective action

In this section, we provide a microscopic derivation of the low-energy effective action for a bilayer superconductor with interlayer Josephson coupling. By integrating out the fermionic degrees of freedom within the path-integral approach [1, 2], we obtain a controlled description of the Josephson phase dynamics and the associated collective fluctuations.

Specifically, based on the Hamiltonian presented in the main text, the action of the model is given by

$$S = \int dx \sum_{j=1,2} \left[\sum_{s=\uparrow,\downarrow} \psi_{js}^\dagger(x) (i\partial_t - \xi_{j\hat{\mathbf{p}}}) \psi_{js}(x) - \Delta_j(x) \psi_{j\uparrow}^\dagger(x) \psi_{j\downarrow}^\dagger(x) - \Delta_j^*(x) \psi_{j\downarrow}(x) \psi_{j\uparrow}(x) + \frac{|\Delta_j(x)|^2}{U} \right] - \frac{1}{2} \int dx dx' \sum_j V_{jj}(x-x') \rho_j^\dagger(x) \rho_j(x) - \frac{1}{2} \int dx dx' \sum_j V_{12}(x-x') [\rho_1^\dagger(x) \rho_2(x) + \rho_2^\dagger(x) \rho_1(x)] + S_{\text{JC}}, \quad (\text{S1})$$

where the interlayer Josephson-coupling part is [3–5]

$$S_{\text{JC}} = \int dx \left\{ \frac{1}{2} (J_1 \Delta_1 \Delta_2^* + J_1^* \Delta_2 \Delta_1^*) + \frac{1}{2} [J_2 (\Delta_1 \Delta_2^*)^2 + J_2^* (\Delta_2 \Delta_1^*)^2] \right\}. \quad (\text{S2})$$

Here, $\psi_{js}(x)$ is the fermionic field in layer j with spin s ; $x = (t, \mathbf{x})$ denotes the spacetime coordinate (a four-vector in relativistic notation); $\hat{\mathbf{p}} = -i\hbar\nabla$ is the momentum operator; $U < 0$ is the attractive pairing interaction. The density operator is $\rho_j(x) = \sum_s \psi_{js}^\dagger(x) \psi_{js}(x)$. For simplicity and without loss of generality, we assume a parabolic dispersion $\xi_{j\hat{\mathbf{p}}} = \hat{\mathbf{p}}^2/(2m) - \mu$ (identical in the two layers). The long-range Coulomb interaction contains both intralayer contributions $V_{11}(x-x') = V_{22}(x-x')$ and an interlayer term $V_{12}(x-x')$. In momentum space they take the form [6]

$$V_{jj}(q) = \frac{2\pi e^2}{\varepsilon q}, \quad V_{12}(q) = \frac{2\pi e^2}{\varepsilon q} e^{-qd}, \quad (\text{S3})$$

where d is the interlayer separation and ε denotes the background dielectric constant.

The superconducting order parameter in each layer is parameterized as [1, 7]

$$\Delta_j(x) = |\Delta_j| e^{i\phi_j(x)}, \quad (\text{S4})$$

where $|\Delta_j|$ and $\phi_j(x)$ denotes the superconducting gap and phase, respectively.

The interlayer Josephson coupling is assumed to contain both the conventional first harmonic and a higher-order second harmonic contribution, with generally complex amplitudes J_1 and J_2 [3–5]. Here we do not repeat the microscopic derivation of these terms, which can be obtained from standard tunneling-Hamiltonian treatments and higher-order perturbation theory in the interlayer hopping amplitude [8, 9]. Notably, in standard microscopic derivations of the Josephson effect [8, 9], these terms originate from interlayer electron hopping, which mediates tunneling of Cooper pairs between the two superconducting layers. The first harmonic J_1 corresponds to the lowest-order tunneling of a single Cooper pair, while the second harmonic J_2 naturally appears from higher-order processes involving correlated tunneling of two Cooper pairs via virtual intermediate states [8]. Here we take this form as a starting point and further examine the implications of phase coherence.

* fzy5099@psu.edu

† lqc3@psu.edu

Then, applying the Hubbard-Stratonovich transformation for long-range coulomb interactions and using the unitary transformation $\psi_{js}(x) \rightarrow e^{i\phi_j(x)/2}\psi_{js}(x)$ [10–13], the action becomes

$$\begin{aligned}
S = & \int dx \left[\sum_{s=\uparrow,\downarrow} \psi_{1s}^\dagger(x) [i\partial_t - \partial_t \phi_1(x)/2 - \xi_{\mathbf{p}+\nabla} \phi_1/2 - \mu_+(x) - \mu_-(x)] \psi_{1s}(x) - |\Delta_1| \psi_{1\uparrow}^\dagger(x) \psi_{1\downarrow}^\dagger(x) - |\Delta_1| \psi_{1\downarrow}(x) \psi_{1\uparrow}(x) + \frac{|\Delta_1|^2}{U} \right] \\
& + \int dx \left[\sum_{s=\uparrow,\downarrow} \psi_{2s}^\dagger(x) [i\partial_t - \partial_t \phi_2(x)/2 - \xi_{\mathbf{p}+\nabla} \phi_2/2 - \mu_+(x) + \mu_-(x)] \psi_{2s}(x) - |\Delta_2| \psi_{2\uparrow}^\dagger(x) \psi_{2\downarrow}^\dagger(x) - |\Delta_2| \psi_{2\downarrow}(x) \psi_{2\uparrow}(x) + \frac{|\Delta_2|^2}{U} \right] \\
& + \int dt d\mathbf{q} \frac{2|\mu_+(t, \mathbf{q})|^2}{V_+(q)} + \int dt d\mathbf{q} \frac{2|\mu_-(t, \mathbf{q})|^2}{V_-(q)} + S_{\text{JC}}, \tag{S5}
\end{aligned}$$

Here, $\mu_\pm(x)$ denotes the Coulomb-interaction-related Hartree field; the symmetric channel $V_+(q) = \frac{2\pi e^2}{\varepsilon q} (1 + e^{-qd})$ describes the long-range Coulomb interaction associated with total charge fluctuations, while the antisymmetric channel $V_-(q) = \frac{2\pi e^2}{\varepsilon q} (1 - e^{-qd})$ governs interlayer charge transfer modes [6].

We introduce the relative (Josephson) and total superconducting phase fields as (in analogy with the derivation of the Leggett mode [14])

$$\phi(x) = \phi_1(x) - \phi_2(x), \tag{S6}$$

$$\theta(x) = [\phi_1(x) + \phi_2(x)]/2. \tag{S7}$$

and, restrict to the symmetric case

$$|\Delta_1| = |\Delta_2| = |\Delta|,$$

for which the two layers are identical at the mean-field level and differ only through phase and scalar-potential fluctuations. In this case, in Nambu space and neglecting total-derivative (boundary) terms [2], the action becomes

$$\begin{aligned}
S = & \int dx \left\{ \Psi_1^\dagger(x) [G^{-1} - \Sigma_1] \Psi_1(x) - \frac{1}{2m} \left[\nabla \left(\frac{2\theta + \phi}{4} \right) \right]^2 + \frac{|\Delta|^2}{U} \right\} + \int dx \left\{ \Psi_2^\dagger(x) [G^{-1} - \Sigma_2] \Psi_2(x) - \frac{1}{2m} \left[\nabla \left(\frac{2\theta - \phi}{4} \right) \right]^2 + \frac{|\Delta|^2}{U} \right\} \\
& + \int dt d\mathbf{q} \frac{2|\mu_+(t, \mathbf{q})|^2}{V_+(q)} + \int dt d\mathbf{q} \frac{2|\mu_-(t, \mathbf{q})|^2}{V_-(q)} + S_{\text{JC}}, \tag{S8}
\end{aligned}$$

where the Nambu spinor $\Psi_j^\dagger = (\psi_{j\uparrow}^\dagger, \psi_{j\downarrow}^\dagger)$; the bare inverse Nambu Green's function

$$G^{-1} = i\partial_t - \xi_{\mathbf{k}} \tau_3 - |\Delta| \tau_1 - \mathbf{v}_{\mathbf{k}} \cdot \mathbf{p}_s, \tag{S9}$$

with $\mathbf{p}_s = \nabla \theta/2$, and the self-energy corrections are

$$\Sigma_1 = \frac{\partial_t \theta(x)}{2} \tau_3 + \frac{\partial_t \phi(x)}{4} \tau_3 + \mu_+ \tau_3 + \mu_- \tau_3 + \frac{1}{2m} \left[\nabla \left(\frac{2\theta + \phi}{4} \right) \right]^2 \tau_3 + \frac{\mathbf{v}_{\mathbf{k}} \cdot \nabla \phi}{4}, \tag{S10}$$

$$\Sigma_2 = \frac{\partial_t \theta(x)}{2} \tau_3 - \frac{\partial_t \phi(x)}{4} \tau_3 + \mu_+ \tau_3 - \mu_- \tau_3 + \frac{1}{2m} \left[\nabla \left(\frac{2\theta - \phi}{4} \right) \right]^2 \tau_3 - \frac{\mathbf{v}_{\mathbf{k}} \cdot \nabla \phi}{4}. \tag{S11}$$

The fermionic degrees of freedom can now be integrated out exactly, yielding the effective action

$$\begin{aligned}
S_{\text{eff}} = & \int dx \left(\bar{\text{Tr}} \ln G^{-1} - \sum_n \frac{1}{n} \bar{\text{Tr}} (\Sigma_1 G)^n \right) + \int dx \left(\bar{\text{Tr}} \ln G^{-1} - \sum_n \frac{1}{n} \bar{\text{Tr}} (\Sigma_2 G)^n \right) - \int dx \left[\frac{1}{m} \left(\frac{\nabla \theta}{2} \right)^2 + \frac{1}{m} \left(\frac{\nabla \phi}{4} \right)^2 \right] \\
& + 2 \int dx \frac{|\Delta|^2}{U} + \int dt d\mathbf{q} \frac{2|\mu_+(t, \mathbf{q})|^2}{V_+(q)} + \int dt d\mathbf{q} \frac{2|\mu_-(t, \mathbf{q})|^2}{V_-(q)} + S_{\text{JC}}, \tag{S12}
\end{aligned}$$

where the fermionic Green function in the Matsubara representation and momentum space is given by [1, 7, 8]

$$G(p) = \frac{ip_n \tau_0 - \mathbf{p}_s \cdot \mathbf{v}_{\mathbf{k}} \tau_0 + \xi_{\mathbf{k}} \tau_3 + |\Delta| \tau_1}{(ip_n - E_{\mathbf{k}}^+) (ip_n - E_{\mathbf{k}}^-)}. \tag{S13}$$

Here, the quasiparticle spectrum acquires a Doppler shift $\mathbf{v}_{\mathbf{k}} \cdot \mathbf{p}_s$ [11, 13, 15–17] and takes the form $E_{\mathbf{k}}^\pm = \mathbf{v}_{\mathbf{k}} \cdot \mathbf{p}_s \pm E_{\mathbf{k}}$ where $E_{\mathbf{k}} = \sqrt{\xi_{\mathbf{k}}^2 + |\Delta|^2}$ is the Bogoliubov dispersion.

Retaining the lowest two orders (i.e., $n = 1$ and $n = 2$) and neglecting total-derivative (boundary) terms yield

$$\begin{aligned}
S_{\text{eff}} &= 2 \int dR \left\{ \sum_{p_n, \mathbf{k}} \ln[(ip_n - E_{\mathbf{k}}^+)(ip_n - E_{\mathbf{k}}^-)] + \frac{|\Delta|^2}{U} - \frac{\bar{\chi}_3}{2m} \left(\frac{\nabla\theta}{2} \right)^2 - \frac{\bar{\chi}_3}{2m} \left(\frac{\nabla\phi}{4} \right)^2 - \chi_{00} \frac{v_F^2}{2} \left(\frac{\nabla\phi}{4} \right)^2 \right\} \\
&\quad - \int dR \chi_{33} \left\{ \left[\frac{\partial_t \theta(x)}{2} + \frac{\partial_t \phi(x)}{4} + \mu_+ + \mu_- \right]^2 + \left[\frac{\partial_t \theta(x)}{2} - \frac{\partial_t \phi(x)}{4} + \mu_+ - \mu_- \right]^2 \right\} \\
&\quad + \int dt d\mathbf{q} \frac{2|\mu_+(t, \mathbf{q})|^2}{V_+(q)} + \int dt d\mathbf{q} \frac{2|\mu_-(t, \mathbf{q})|^2}{V_-(q)} + S_{\text{JC}} \\
&= 2 \int dR \left\{ \sum_{p_n, \mathbf{k}} \ln[(ip_n - E_{\mathbf{k}}^+)(ip_n - E_{\mathbf{k}}^-)] + \frac{|\Delta|^2}{U} - \frac{\bar{\chi}_3}{2m} \left(\frac{\nabla\theta}{2} \right)^2 - \frac{\bar{\chi}_3}{2m} \left(\frac{\nabla\phi}{4} \right)^2 - \chi_{00} \frac{v_F^2}{2} \left(\frac{\nabla\phi}{4} \right)^2 \right\} \\
&\quad - 2 \int dR \chi_{33} \left\{ \left[\frac{\partial_t \theta(x)}{2} + \mu_+ \right]^2 + \left[\frac{\partial_t \phi(x)}{4} + \mu_- \right]^2 \right\} + \int dt d\mathbf{q} \frac{2|\mu_+(t, \mathbf{q})|^2}{V_+(q)} + \int dt d\mathbf{q} \frac{2|\mu_-(t, \mathbf{q})|^2}{V_-(q)} + S_{\text{JC}}, \quad (\text{S14})
\end{aligned}$$

with the correlation coefficients,

$$\tilde{\chi}_3 = \sum_{\mathbf{k}} \left[1 + \sum_{p_n} \text{Tr}[G_0(p)\tau_3] \right] = \sum_{\mathbf{k}} \left[1 + \frac{\xi_{\mathbf{k}}}{E_{\mathbf{k}}} (f(E_{\mathbf{k}}^+) - f(E_{\mathbf{k}}^-)) \right] = -\frac{k_F^2}{2m} \sum_{\mathbf{k}} \partial_{\xi_{\mathbf{k}}} \left[\frac{\xi_{\mathbf{k}}}{E_{\mathbf{k}}} (f(E_{\mathbf{k}}^+) - f(E_{\mathbf{k}}^-)) \right] = n, \quad (\text{S15})$$

$$\chi_{03} = \frac{1}{2} \sum_p \text{Tr}[G_0(p)\tau_0 G_0(p)\tau_3] = 0, \quad (\text{S16})$$

$$\chi_{33} = \frac{1}{2} \sum_p \text{Tr}[G_0(p)\tau_3 G_0(p)\tau_3] = \sum_{p_n, \mathbf{k}} \frac{(ip_n - \mathbf{p}_s \cdot \mathbf{v}_{\mathbf{k}})^2 + \xi_{\mathbf{k}}^2 - |\Delta|^2}{(ip_n - E_{\mathbf{k}}^+)^2 (ip_n - E_{\mathbf{k}}^-)^2} = \sum_{\mathbf{k}} \partial_{\xi_{\mathbf{k}}} \left[\frac{\xi_{\mathbf{k}}}{2E_{\mathbf{k}}} (f(E_{\mathbf{k}}^+) - f(E_{\mathbf{k}}^-)) \right] = -D, \quad (\text{S17})$$

$$\chi_{00} = \frac{1}{2} \sum_p \text{Tr}[G_0(p)G_0(p)] = \sum_{p_n, \mathbf{k}} \frac{(ip_n - \mathbf{p}_s \cdot \mathbf{v}_{\mathbf{k}})^2 + \xi_{\mathbf{k}}^2 + |\Delta|^2}{(ip_n - E_{\mathbf{k}}^+)^2 (ip_n - E_{\mathbf{k}}^-)^2} = \sum_{\mathbf{k}} \partial_{E_{\mathbf{k}}} \left[\frac{f(E_{\mathbf{k}}^+) - f(E_{\mathbf{k}}^-)}{2} \right]. \quad (\text{S18})$$

Here, n is carrier density and D is the density of states of carriers; $R = (t, \mathbf{R})$ denotes the center-of-mass coordinate [1, 11], where \mathbf{R} is confined to the 2D in-plane space of each layer.

Integrating out the Hartree fields yields the effective action for the gap and phase fluctuations:

$$\begin{aligned}
S_{\text{eff}} &= 2 \int dR \left\{ \sum_{p_n, \mathbf{k}} \ln[(ip_n - E_{\mathbf{k}}^+)(ip_n - E_{\mathbf{k}}^-)] + \frac{|\Delta|^2}{U} - \frac{np_s^2}{2m} \right\} + 2 \int dt d\mathbf{q} \left\{ \frac{D}{1 + DV_+(q)} \left[\frac{\partial_t \theta(t, \mathbf{q})}{2} \right]^2 \right\} \\
&\quad + 2 \int dt d\mathbf{q} \left\{ \frac{D}{1 + DV_-(q)} \left[\frac{\partial_t \phi(t, \mathbf{q})}{4} \right]^2 \right\} - 2 \int dR \frac{f_s}{2} \left(\frac{\nabla\phi}{4} \right)^2 + S_{\text{JC}}, \quad (\text{S19})
\end{aligned}$$

where the superfluid stiffness can be expressed as

$$\begin{aligned}
f_s &= \frac{\chi_3}{m} + v_F^2 \chi_{00} = v_F^2 \sum_{\mathbf{k}} \left\{ \partial_{E_{\mathbf{k}}} \left[\frac{f(E_{\mathbf{k}}^+) - f(E_{\mathbf{k}}^-)}{2} \right] - \partial_{\xi_{\mathbf{k}}} \left[\frac{\xi_{\mathbf{k}}}{2E_{\mathbf{k}}} (f(E_{\mathbf{k}}^+) - f(E_{\mathbf{k}}^-)) \right] \right\} = v_F^2 \sum_{\mathbf{k}} \frac{|\Delta|^2}{E_{\mathbf{k}}} \left[\frac{f(E_{\mathbf{k}}^+) - f(E_{\mathbf{k}}^-)}{2E_{\mathbf{k}}} \right] \\
&\approx v_F^2 |\Delta|^2 \sum_{\mathbf{k}} \frac{f(E_{\mathbf{k}}^-) - f(E_{\mathbf{k}}^+)}{2E_{\mathbf{k}}^3}. \quad (\text{S20})
\end{aligned}$$

In the long-wavelength limit, one has

$$V_+(q) = \frac{2\pi e^2}{\varepsilon q} (1 + e^{-qd}) \approx \frac{4\pi e^2}{\varepsilon q} = 2V_{2\text{D}}(q), \quad V_-(q) = \frac{2\pi e^2}{\varepsilon q} (1 - e^{-qd}) \approx \frac{2\pi e^2 d}{\varepsilon}, \quad (\text{S21})$$

and then, the effective action is simplified to

$$S_{\text{eff}} = S_{\text{intra}}(|\Delta|, \mathbf{p}_s^2) + S_J(\phi). \quad (\text{S22})$$

where the intralayer contribution reads

$$S_{\text{intra}}(|\Delta|, \mathbf{p}_s^2) = 2 \int dR \left\{ \sum_{p_n, \mathbf{k}} \ln[(ip_n - E_{\mathbf{k}}^+)(ip_n - E_{\mathbf{k}}^-)] + \frac{|\Delta|^2}{U} - \frac{np_s^2}{2m} \right\} + 2 \int dt d\mathbf{q} \left\{ \frac{D}{1 + 2DV_{2\text{D}}(q)} \left[\frac{\partial_t \theta(t, \mathbf{q})}{2} \right]^2 \right\} \quad (\text{S23})$$

while the Josephson contribution is given by

$$S_J(\phi) = \int dR \left[\frac{D_l}{2} \left(\frac{\partial_t \phi}{2} \right)^2 - \frac{f_s}{4} \left(\frac{\nabla \phi}{2} \right)^2 + |J_1| |\Delta|^2 \cos(\phi + \alpha) + |J_2| |\Delta|^4 \cos(2\phi) \right], \quad (\text{S24})$$

with $D_l = D/(1 + D2\pi e^2 d/\epsilon)$ being the effective density of states renormalized by the interlayer Coulomb interaction.

The intralayer sector here coincides with the standard effective action of a two-dimensional superconductor and governs the intralayer superconducting properties [11, 18–20]. These contributions will be discussed in Sec. SIII. In contrast, the Josephson sector $S_J(\phi)$ controls the equilibrium configuration and dynamical behavior of the relative phase between the two layers, which will be analyzed in Sec. SII. The resulting superfluid stiffness derived here is fully consistent with those obtained from Gor'kov theory, kinetic formulations, and current–current correlation approaches [6, 7, 11–13, 21].

1. Inclusion of disorder

The above derivation holds in the clean limit. In practice, disorder is unavoidable in monolayer systems and affects the gap and phase (stiffness) sectors in qualitatively different ways. For isotropic s -wave pairing in the diffusive limit, nonmagnetic disorder does not directly modify the gap equation, in accordance with Anderson's theorem. Instead, disorder influences the superconducting state primarily through the renormalization of the superfluid phase stiffness. This conclusion has been consistently established using multiple theoretical frameworks, including Gor'kov formalism [7], Eilenberger transport theory [22–24], gauge-invariant kinetic equations [13], and diagrammatic approaches incorporating vertex corrections in the current–current response [21, 24]. The essential reason is that the superfluid stiffness is determined by the transverse current–current response kernel. In the presence of impurity scattering, vertex corrections necessarily enter this kernel and lead to a suppression of the stiffness by elastic scattering processes.

To incorporate this effect without explicitly solving the fully impurity-dressed response functions, one may adopt the well-established clean-to-dirty interpolation introduced by Tinkham [25]. This interpolation relates the penetration depth via $\lambda^2 = \lambda_{\text{clean}}^2 (1 + \xi/l)$, which implies $n_s \rightarrow n_{s,\text{clean}}/(1 + \xi/l)$. This approach recovers the Mattis–Bardeen dirty-limit behavior [26, 27], connects smoothly to finite-scattering extensions [28], quantitatively captures penetration-depth measurements across disorder regimes in conventional superconductors [29–32], and is further supported by fully microscopic derivations. Then, the superfluid stiffness takes the form

$$f_s = \frac{v_F^2 |\Delta|^2}{1 + \xi/l} \sum_{\mathbf{k}} \frac{f(E_{\mathbf{k}}^-) - f(E_{\mathbf{k}}^+)}{2E_{\mathbf{k}}^3}, \quad (\text{S25})$$

where $\xi = \hbar v_F / |\Delta|$ is the coherence length and $l = v_F \tau$ is the mean free path with τ being the effective scattering time.

SII. Derivation of Josephson fluctuations

In this section, we derive the effective Josephson dynamics in the presence of phase fluctuations from a microscopic perspective. Specifically, we decompose the Josephson phase as

$$\phi = \phi_e + \delta\phi(R), \quad (\text{S26})$$

where ϕ_e denotes the equilibrium phase configuration, and $\delta\phi(R)$ describes dynamical fluctuations around this equilibrium. Substituting this decomposition into the Josephson-phase action enables a systematic and self-consistent separation between the static equilibrium configuration and the dynamical fluctuations. Most importantly, this procedure allows us to bosonize the Josephson phase fluctuations and treat them as collective bosonic modes, thereby capturing fluctuation-induced renormalizations of the Josephson response in a controlled, fully microscopic framework that goes beyond both mean-field approximations and phenomenological descriptions.

A. Equilibrium configuration

Substituting the decomposition [Eq. (S26)] into the Josephson-phase-related action $S_J(\phi)$ [Eq. (S24)], the optimal equilibrium phase ϕ_e^{op} is determined by minimizing the static Josephson energy obtained from the potential part of the action,

$$E_J(\phi_e) = -|J_1| |\Delta|^2 \langle \cos(\phi + \alpha) \rangle - |J_2| |\Delta|^4 \langle \cos(2\phi) \rangle. \quad (\text{S27})$$

Using the statistic average $\langle \delta\phi \rangle = 0$ and $\langle \delta\phi^2 \rangle \neq 0$, the thermal average can be evaluated via the cumulant expansion [2, 7, 8],

$$\begin{aligned} \langle \cos(m\phi) \rangle &= \text{Re}[e^{im\phi_e} \langle e^{im\delta\phi} \rangle] = \text{Re}\left[e^{im\phi_e} \sum_{n=0}^{\infty} \frac{\langle (im\delta\phi)^{2n} \rangle}{(2n)!}\right] = \text{Re}\left[e^{im\phi_e} \sum_{n=0}^{\infty} \frac{(2n-1)!!(-1)^n m^{2n} \langle \delta\phi^2 \rangle^n}{(2n)!}\right] \\ &= \text{Re}\left[e^{im\phi_e} \sum_{n=0}^{\infty} \frac{(-1)^n m^{2n} \langle \delta\phi^2 \rangle^n}{2^n n!}\right] = \text{Re}\left[e^{im\phi_e} e^{-\langle \delta\phi^2 \rangle / 2}\right] = \cos(m\phi_e) e^{-m^2 \langle \delta\phi^2 \rangle / 2}. \end{aligned} \quad (\text{S28})$$

As a result, the fluctuation-renormalized Josephson energy becomes

$$E_J(\phi_e) = -\bar{J}_1(T) \cos(\phi_e + \alpha) - \bar{J}_2(T) \cos(2\phi_e), \quad (\text{S29})$$

where the effective Josephson couplings are renormalized by Josephson phase fluctuations as

$$\bar{J}_1(T) = |J_1| |\Delta(T)|^2 \exp[-\langle \delta\phi^2(T) \rangle / 2], \quad (\text{S30})$$

$$\bar{J}_2(T) = |J_2| |\Delta(T)|^4 \exp[-2\langle \delta\phi^2(T) \rangle]. \quad (\text{S31})$$

Consequently, as rigorously demonstrated above, the optimal equilibrium phase ϕ_e^{op} is determined by minimizing the fluctuation-renormalized Josephson energy rather than the bare one,

$$\phi_e^{\text{op}} = \arg \min_{\phi_e \in [0, 2\pi)} E_J(\phi_e), \quad (\text{S32})$$

suggesting the nontrivial impact of phase fluctuations on the equilibrium configuration.

1. Josephson current

In the presence of an externally imposed dc Josephson current I_J , the thermodynamic potential acquires an additional work term associated with the phase bias. The effective Josephson energy is therefore modified to [8]

$$\tilde{E}_J(\phi_e) = -\bar{J}_1(T) \cos(\phi_e + \alpha) - \bar{J}_2(T) \cos(2\phi_e) - \frac{I_J}{2e} \phi_e, \quad (\text{S33})$$

The equilibrium phase under a finite current is determined by minimizing $\tilde{E}_J(\phi_e)$. This yields the generalized current–phase relation

$$I_J(\phi_e) = 2e[\bar{J}_1(T) \sin(\phi_e + \alpha) + 2\bar{J}_2(T) \sin(2\phi_e)]. \quad (\text{S34})$$

The phase fluctuations thus renormalize not only the Josephson energy but also the current–phase relation, suppressing both harmonic components exponentially via the Debye–Waller-like factors [33, 34].

Particularly, higher-order Josephson couplings are suppressed more strongly than the lowest-order term: the second-harmonic coupling $\bar{J}_2 \propto \exp(-2\langle \delta\phi^2 \rangle)$ decays parametrically faster than the first-harmonic coupling $\bar{J}_1 \propto \exp(-\langle \delta\phi^2 \rangle / 2)$ as phase fluctuations increase with temperature. Thus, non-sinusoidal components of the Josephson current–phase relation are particularly fragile against phase decoherence, with higher-order harmonics expected to be even more fragile. As the Josephson diode nonreciprocity heavily relies on these non-sinusoidal components [3–5], the Josephson diode effect is expected to disappear at a temperature lower than the critical temperature where the Josephson critical current is suppressed.

B. Dynamics of Josephson phase fluctuations

Then, we derive the dynamics of the Josephson phase fluctuations. Starting from Eq. (S24) and the decomposition in Eq. (S26), the Euler–Lagrange equation with respect to the phase fluctuation field $\delta\phi$ reads [2]

$$\partial_\mu \left[\frac{\partial S_J[\phi]}{\partial (\partial_\mu \delta\phi / 2)} \right] = \frac{\partial S_J[\phi]}{\partial (\delta\phi / 2)}, \quad (\text{S35})$$

which leads to the equation of motion

$$[D_I \partial_t^2 - f_s \nabla^2 / 2] \delta\phi / 2 + 2|J_1| |\Delta|^2 \sin(\phi_e + \delta\phi + \alpha) + 4|J_2| |\Delta|^4 \sin(2\phi_e + 2\delta\phi) = 0. \quad (\text{S36})$$

To proceed, we treat the phase fluctuations within a field-theoretical cumulant expansion [2, 7], retaining only a single phase operator while contracting the remaining fields. Using the trigonometric identity

$$\sin(m\phi_e + m\delta\phi) = \sin m\phi_e \cos m\delta\phi + \cos m\phi_e \sin m\delta\phi, \quad (\text{S37})$$

and assuming $\langle \delta\phi \rangle = 0$, the critical response in the equation of motion is governed by the second contribution. The sine of the phase fluctuation is expanded as

$$\sin m\delta\phi(R) = \sum_{n=0}^{\infty} \frac{(-1)^n m^{2n+1}}{(2n+1)!} \delta\phi^{2n+1}(R). \quad (\text{S38})$$

Within the cumulant approximation [2, 7, 8], we retain only a single uncontracted phase operator while contracting the remaining $2n$ fields according to Wick's theorem [2],

$$\delta\phi^{2n+1}(R) \rightarrow (2n-1)!! \langle \delta\phi^2(R) \rangle^n \delta\phi(R). \quad (\text{S39})$$

Substituting this back, we obtain

$$\begin{aligned} \sin \delta\phi(R) &\rightarrow \sum_{n=0}^{\infty} \frac{(-1)^n m^{2n+1}}{(2n+1)!} (2n-1)!! \langle \delta\phi^2(R) \rangle^n \delta\phi(R) \\ &= \sum_{n=0}^{\infty} \frac{(-1)^n m^{2n+1}}{2^n n!} \langle \delta\phi^2(R) \rangle^n \delta\phi(R) = \exp\left[-\frac{m^2}{2} \langle \delta\phi^2 \rangle\right] m\delta\phi(R). \end{aligned} \quad (\text{S40})$$

Then, the equation of motion of the Josephson phase fluctuations reads

$$\left[D_I \partial_t^2 - f_s \nabla^2 / 2 + 4|J_1| |\Delta|^2 \exp(-\langle \delta\phi^2 \rangle / 2) \cos(\phi_e + \alpha) + 16|J_2| |\Delta|^4 \exp(-2\langle \delta\phi^2 \rangle) \cos(2\phi_e) \right] \frac{\delta\phi(R)}{2} = 0, \quad (\text{S41})$$

or equivalently,

$$\left[D_I \partial_t^2 - f_s \nabla^2 / 2 + 4\bar{J}_1 \cos(\phi_e + \alpha) + 16\bar{J}_2 \cos(2\phi_e) \right] \frac{\delta\phi}{2} = 0. \quad (\text{S42})$$

From this equation, the energy spectrum of the collective Josephson phase mode follows as

$$D_I \omega_L^2(q) = 4\bar{J}_1 \cos(\phi_e^{\text{op}} + \alpha) + 16\bar{J}_2 \cos(2\phi_e^{\text{op}}) + f_s q^2 / 2. \quad (\text{S43})$$

Clearly, the interlayer Josephson coupling opens a finite gap in the collective excitation spectrum by locking the relative phase, in agreement with the Leggett-type phase mode [6, 14].

In particular, the renormalized Josephson couplings $\bar{J}_1(T)$ and $\bar{J}_2(T)$ entering the excitation gap explicitly encode the feedback between thermal phase fluctuations and Josephson coherence. As temperature increases, the growth of the thermal phase fluctuation $\langle \delta\phi^2(T) \rangle$ leads to an exponential suppression of $\bar{J}_{1,2}(T)$ through the Debye–Waller-like factor, while the reduction of the pairing amplitude $|\Delta(T)|$ further suppresses the couplings via their explicit amplitude dependence. The resulting decrease in Josephson stiffness produces a progressive softening of the phase mode upon warming. The softened mode in turn enhances Josephson phase fluctuations, establishing a self-consistent feedback mechanism.

C. Statistic average of Josephson phase fluctuations

From the equation of motion of the Josephson phase fluctuations in Eq. (S42), the average of Josephson phase fluctuations can be obtained within the quantum-statistic mechanism [7, 8] either via the fluctuation–dissipation theorem or within the Matsubara formalism. The two approaches are fully equivalent and yield identical results,

$$\langle \delta\phi^2(T) \rangle = \int \frac{2d\mathbf{q}}{(2\pi)^2} \frac{2n_B[\omega_L(q)] + 1}{D_I \omega_L(q)}, \quad (\text{S44})$$

reflecting the bosonic description of the phase degree of freedom as a collective phase mode.

Fluctuation dissipation theorem.—Considering the thermal fluctuations, the dynamics of the phase from Eq. (S42) is given by

$$\left[D_I \omega_L^2(\mathbf{q}) - \omega^2 + iD_I \omega \gamma \right] \frac{\delta\phi(\omega, \mathbf{q})}{2} = J_{\text{th}}(\omega, \mathbf{q}). \quad (\text{S45})$$

Here, we have introduced a thermal field $J_{\text{th}}(\omega, \mathbf{q})$ that obeys the fluctuation-dissipation theorem [35]:

$$\langle J_{\text{th}}(\omega, \mathbf{q}) J_{\text{th}}^*(\omega', \mathbf{q}') \rangle = \frac{(2\pi)^3 D_l \gamma \omega \delta(\omega - \omega') \delta(\mathbf{q} - \mathbf{q}')}{\tanh(\beta\omega/2)}, \quad (\text{S46})$$

and $\gamma = 0^+$ is a phenomenological damping constant. From this dynamics, the average of the phase fluctuations is given by

$$\begin{aligned} \frac{1}{4} \langle \delta\phi^2 \rangle &= \int \frac{d\omega d\omega' d\mathbf{q} d\mathbf{q}'}{(2\pi)^6} \frac{\langle J_{\text{th}}(\omega, \mathbf{q}) J_{\text{th}}^*(\omega', \mathbf{q}') \rangle}{D_l^2 [(\omega^2 - \omega_L^2(\mathbf{q})) - i\omega\gamma] [(\omega'^2 - \omega_L^2(\mathbf{q}')) + i\omega'\gamma]} = \int \frac{d\omega d\mathbf{q}}{D_l (2\pi)^2} \frac{\gamma\omega/\tanh(\beta\omega/2)}{[\omega^2 - \omega_L^2(\mathbf{q})]^2 + \omega^2\gamma^2} \\ &= \int \frac{d\mathbf{q}}{(2\pi)^2} \frac{[2n_B(\omega_L(\mathbf{q})) + 1]}{2D_l\omega_L(\mathbf{q})}. \end{aligned} \quad (\text{S47})$$

Matsubara formalism.—Within the Matsubara formalism, by mapping into the imaginary-time space, from Eq. (S42), the thermal phase fluctuation reads [7]

$$\begin{aligned} \frac{1}{4} \langle \delta\phi^2 \rangle &= \int \frac{d\mathbf{q}}{(2\pi)^2} \left[\left\langle \left| \frac{\delta\phi^*(\tau, \mathbf{q})}{2} \frac{\delta\phi(\tau, \mathbf{q})}{2} e^{-\int_0^\beta d\tau d\mathbf{q} D_l \delta\phi^*(\tau, \mathbf{q}) (\omega_L^2(\mathbf{q}) - \partial_\tau^2) \delta\phi(\tau, \mathbf{q})/4} \right| \right] \right] \\ &= \int \frac{d\mathbf{q}}{(2\pi)^2} \left[\frac{1}{\mathcal{Z}_0} \int D\delta\phi D\delta\phi^* \frac{\delta\phi^*(\tau, \mathbf{q})}{2} \frac{\delta\phi(\tau, \mathbf{q})}{2} e^{-\int_0^\beta d\tau d\mathbf{q} D_l \delta\phi^*(\tau, \mathbf{q}) (\omega_L^2(\mathbf{q}) - \partial_\tau^2) \delta\phi(\tau, \mathbf{q})/4} \right] \\ &= \int \frac{d\mathbf{q}}{(2\pi)^2} \frac{1}{\mathcal{Z}_0} \int D\delta\phi D\delta\phi^* \delta_{J_q^*} \delta_{J_q} e^{-\int_0^\beta d\tau d\mathbf{q} [D_l \delta\phi^*(\tau, \mathbf{q}) (\omega_L^2(\mathbf{q}) - \partial_\tau^2) \delta\phi(\tau, \mathbf{q})/4 + J_q \delta\phi(\mathbf{q})/2 + J_q^* \delta\phi^*(\mathbf{q})/2]} \Big|_{J=J^*=0} \\ &= \int \frac{d\mathbf{q}}{(2\pi)^2} \frac{1}{D_l} \delta_{J_q^*} \delta_{J_q} \exp \left\{ - \int_0^\beta d\tau \sum_{q'} J_{q'} \frac{1}{\partial_\tau^2 - \omega_L^2(\mathbf{q})} J_{q'}^* \right\} \Big|_{J=J^*=0} = - \int \frac{d\mathbf{q}}{(2\pi)^2} \frac{1}{\beta} \sum_{\omega_n} \frac{1}{D_l (i\Omega_n)^2 - \omega_L^2(\mathbf{q})} \\ &= \int \frac{d\mathbf{q}}{(2\pi)^2} \frac{2n_B(\omega_L(\mathbf{q})) + 1}{2D_l\omega_L(\mathbf{q})}, \end{aligned} \quad (\text{S48})$$

which is exactly the same as the one in Eq. (S47) obtained via the fluctuation dissipation theorem. Here, $\Omega_n = 2n\pi T$ represents the Bosonic Matsubara frequencies; $J_{\mathbf{q}}$ denotes the generating functional and $\delta J_{\mathbf{q}}$ stands for the functional derivative.

III. Intralayer superconducting properties: framework beyond mean-field theory

The effective intralayer action S_{intra} governs the superconducting (SC) properties within each individual layer. From this action, the temperature-dependent gap amplitude $|\Delta(T)|$, the phase-fluctuation correlator $\langle \mathbf{p}_s^2 \rangle$, and the renormalized superfluid stiffness $f_s(T)$ is determined at the fully microscopic level. Within our gauge-invariant formulation [12, 36], the phase fluctuations encoded in $\langle \mathbf{p}_s^2 \rangle$ correspond to the in-phase collective excitation [6, 11, 12], namely the bosonic Nambu–Goldstone (NG) mode associated with spontaneous U(1) symmetry breaking in the superconducting state [37–40]. These fluctuations are coupled with long-range Coulomb interactions in the symmetric channel, as demonstrated in Sec. SI.

In 3D superconductors, the NG mode is rendered dynamically inert due to the Anderson–Higgs mechanism [10, 41, 42], acquiring a plasma gap and therefore not contributing to low-energy thermodynamics. In contrast, in 2D systems, the mode remains gapless and constitutes an active low-energy bosonic excitation [11, 18–20, 43]. As a result, phase fluctuations play a central role in determining the thermodynamic and spectral properties of 2D superconductors. In our recent work on 2D superconductors [18–20], we developed a fully self-consistent framework that incorporates long-wavelength NG-mode fluctuations into the superconducting gap equation in the presence of long-range Coulomb interactions, going beyond the conventional mean-field description. A key feature of this approach is that, although the average superfluid momentum vanishes,

$$\langle \mathbf{p}_s \rangle = 0, \quad (\text{S49})$$

the fluctuation correlator remains finite,

$$\langle \mathbf{p}_s^2 \rangle \neq 0. \quad (\text{S50})$$

These finite fluctuations are carried by *bosonic* NG excitations and enter the fermionic self-energy and gap equation in a self-consistent manner. Consequently, both the superconducting gap $|\Delta(T)|$ and its disappearance temperature T_s acquire nontrivial dependence on the strength of the disorder and the carrier density, reflecting fluctuations-induced renormalization effects beyond the mean-field theory [18–20].

In the present work, we directly adopt this fluctuation-renormalized framework for the in-plane sector. By solving the coupled gap and NG-phase-sector equations self-consistently, we determine the superconducting gap $|\Delta(T)|$ and the renormalized phase stiffness $f_s(T)$. These quantities then serve as the fundamental inputs for the subsequent analysis of interlayer Josephson coupling.

Specifically, the self-consistent gap equation takes the form [11, 18–20]

$$\frac{1}{U} = F(p_s^2, |\Delta|, T) = \sum_{\mathbf{k}} \frac{f(E_{\mathbf{k}}^+) - f(E_{\mathbf{k}}^-)}{2E_{\mathbf{k}}}, \quad (\text{S51})$$

where $f(x)$ is the Fermi distribution function. The quasiparticle spectrum acquires a Doppler shift $\mathbf{v}_{\mathbf{k}} \cdot \mathbf{p}_s$ [11, 13, 15–17] and takes the form

$$E_{\mathbf{k}}^{\pm} = \mathbf{v}_{\mathbf{k}} \cdot \mathbf{p}_s \pm E_{\mathbf{k}}, \quad (\text{S52})$$

with $E_{\mathbf{k}} = \sqrt{\xi_{\mathbf{k}}^2 + |\Delta|^2}$ the Bogoliubov dispersion, $\xi_{\mathbf{k}} = \hbar^2 k^2 / (2m) - \mu$, and $\mathbf{v}_{\mathbf{k}} = \partial_{\mathbf{k}} \xi_{\mathbf{k}}$ the band velocity. In this gauge-invariant formulation, NG phase fluctuations enter the gap equation through the Doppler term in a manner formally analogous to an electromagnetic vector potential [10, 37, 40]. Since the Doppler shift appears linearly but the gap equation involves the symmetric combination $f(E_{\mathbf{k}}^+) - f(E_{\mathbf{k}}^-)$, the leading contribution of phase fluctuations is controlled by the second moment $\langle p_s^2 \rangle$.

The NG fluctuations contribute through the mean-squared superfluid momentum [11, 18–20],

$$\langle p_s^2 \rangle = \int \frac{d\mathbf{q}}{(2\pi)^2} \frac{q^2 [2n_B(\omega_{\text{NG}}) + 1]}{D_q \omega_{\text{NG}}(q)}, \quad (\text{S53})$$

where $n_B(x)$ is the Bose–Einstein distribution. The NG spectrum is given by [11, 18–20]

$$\omega_{\text{NG}}(q) = \sqrt{\frac{f_s q^2}{2D_q}}, \quad (\text{S54})$$

with $D_q = D/[1 + 2DV_{2\text{D}}(q)]$ the Coulomb-renormalized phase stiffness kernel. In the long-wavelength limit, the NG spectrum $\omega_{\text{NG}}(q) \propto \sqrt{q}$, consistent with various theoretical studies of 2D superconductors [6, 10, 11, 43–46].

The superfluid stiffness f_s , obtained from the NG-phase sector, coincides with that derived from the phase-twist (Josephson) response, reflecting the internal consistency of the gauge-invariant formulation. It is expressed as

$$f_s = \frac{v_F^2 |\Delta|^2}{1 + \xi/l} \sum_{\mathbf{k}} \frac{f(E_{\mathbf{k}}^-) - f(E_{\mathbf{k}}^+)}{2E_{\mathbf{k}}^3}, \quad (\text{S55})$$

where $\xi = \hbar v_F / |\Delta|$ is the superconducting coherence length and $l = v_F \tau$ the mean free path (τ is the effective scattering time). The prefactor $(1 + \xi/l)^{-1}$ accounts for disorder-induced renormalization of the phase stiffness.

Consequently, Eqs. (S51)–(S55) form a closed set of coupled self-consistent equations for $\Delta(T)$ and $f_s(T)$. They incorporate fermionic quasiparticle excitations, NG phase fluctuations, and disorder effects on equal footing. The detailed derivation of this framework and its numerical implementation can be found in Refs. [18–20].

One of the important consequences of this framework is that both the zero-temperature gap $|\Delta(0)|$ and the gap-closing temperature T_s become strongly dependent on carrier density and disorder strength once phase fluctuations are incorporated self-consistently. This behavior goes beyond conventional mean-field expectations (Anderson theorem [47–50]), where these quantities are primarily controlled by the pairing interaction alone. In the present framework, long-wavelength NG fluctuations renormalize the quasiparticle spectrum and superfluid stiffness, which in turn feed back into the gap equation. As a result, $|\Delta(0)|$ and T_s acquire nontrivial dependence on carrier density and impurity scattering. As demonstrated in our previous works [18–20], such fluctuation-induced renormalization is consistent with experimental observations in gate-tuned two-dimensional superconductors, including monolayer WTe₂ [51–54], bilayer MoS₂ [55], and thin-film disordered InO_x [56], where both the superconducting gap magnitude and transition scales exhibit pronounced density and disorder dependence.

1. BKT physics

It should be emphasized that Eqs. (S51)–(S55) provide the microscopic input, $|\Delta(T)|$ and $f_s(T)$, for calculating the interlayer Josephson properties and the corresponding out-of-plane transport behavior.

If one is instead interested in in-plane transport properties, the bare stiffness f_s obtained above serves as the initial condition for the standard Berezinskii–Kosterlitz–Thouless (BKT) renormalization-group (RG) flow [36, 57–60]:

$$\frac{dK}{dL} = -K^2 g^2, \quad \frac{dg}{dL} = (2 - K)g, \quad (\text{S56})$$

with initial conditions

$$K(L=0) = \frac{\pi\hbar^2 f_s}{4k_B T}, \quad g(L=0) = 2\pi e^{-c_0 K(L=0)}, \quad (\text{S57})$$

where $c_0 = 2/\pi$ in the two-dimensional limit [18–20]. The fully renormalized superfluid density after vortex screening is

$$\bar{f}_s = \frac{4k_B T}{\pi\hbar^2} K(L=\infty). \quad (\text{S58})$$

For critical behavior in the in-plane sector, the superconducting transition temperature T_c^{intra} is determined by the BKT universal jump condition of the renormalized stiffness \bar{f}_s , while the gap-closing temperature T_s is defined by $\Delta(T_s) = 0$. The in-plane transport properties associated with this BKT criticality have been discussed in detail in our previous works [18–20] and are not the focus of the present study.

Interestingly, since the interlayer Josephson coherence is governed by a distinct, explicitly gapped phase mode, the corresponding transition temperature T_c^{inter} (denoted T_c in the main text) associated with out-of-plane transport does not need to coincide with the in-plane BKT transition temperature T_c^{intra} . This separation of phase-coherence scales provides a natural route to anisotropic superconducting transport behavior and warrants further investigation.

SIV. Simulation treatments

Our numerical analysis consists of two complementary steps which together establish a self-consistent connection between the intralayer superconducting properties and the interlayer Josephson response.

First, following the numerical implementation developed in our previous work, we self-consistently solve Eqs. (S51)–(S55) to obtain the temperature-dependent gap amplitude $|\Delta(T)|$ and superfluid stiffness $f_s(T)$. These quantities serve as the fundamental input for the subsequent interlayer Josephson calculation.

Using this fluctuation-renormalized input, we then self-consistently solve the coupled Josephson equations, Eqs. (S29)–(S32) and Eqs. (S43)–(S44), which determine the optimal equilibrium phase configuration and the thermal average of Josephson phase fluctuations. Once the self-consistent solution is obtained, the current–phase relation is evaluated from Eq. (S34).

The specific parameter values employed in the simulations are summarized in Table SI. With the chosen parameters and in the absence of phase fluctuations (mean-field limit), the zero-temperature superconducting gap is $|\Delta_{\text{MF}}(0)| = 2$ meV, and the Josephson-coupling-induced excitation gap of the interlayer collective mode equals $0.21 |\Delta_{\text{MF}}(0)|$, ensuring that the Josephson collective mode remains well-defined inside the superconducting gap.

TABLE SI. The pairing interaction strength U is chosen such that, in the absence of phase fluctuations (mean-field limit), the zero-temperature superconducting gap satisfies $|\Delta_{\text{MF}}(0)| = 2$ meV. The Debye cutoff energy in the gap equation is taken to be $\omega_D = 6$ meV. The detailed numerical implementation for the intralayer superconducting properties can be found in Refs. [18–20]. The effective mass is set equal to the free electron mass, $m = m_e$. For simplicity, we take the high-energy cutoff for the zero-point contribution of the Josephson bosonic excitations to be the same Debye scale, ω_D . Owing to the Debye–Waller–like exponential structure of the phase-fluctuation renormalization, the zero-point contribution can, in fact, be absorbed into the zero-temperature Josephson parameters $\bar{J}_1(0)$ and $\bar{J}_2(0)$. As a result, the precise value of this ultraviolet cutoff does not affect the temperature dependence or qualitative conclusions of the present work.

$ \Delta_{\text{MF}}(0) $	ω_D	J_1	J_2	α	v_F	$(\tau \Delta_{\text{MF}}(0))^{-1}$
2 meV	6 meV	$16 \text{ meV}^{-1} \mu\text{m}^{-2}$	$1 \text{ meV}^{-3} \mu\text{m}^{-2}$	0.2π	$[0.3, 2] \times 10^5 \text{ m/s}$	$[0, 10]$

The present study predicts that the forward and backward critical currents in low-dimensional Josephson-diode systems, $|I_c^+(T)|$ and $|I_c^-(T)|$, gradually merge as temperature increases, before vanishing simultaneously at T_c . A similar temperature evolution has been reported in several recent experiments (e.g., Refs. [61, 62]). For comparison, we present representative experimental data alongside our theoretical results in Fig. SI. As seen in the figure, the measured temperature dependence exhibits a qualitative trend consistent with our theoretical predictions. Importantly, such temperature-driven merging of $|I_c^+(T)|$ and $|I_c^-(T)|$ does not arise within the conventional single-energy-scale paradigm of Josephson current–phase relations. Instead, it naturally emerges in our framework due to the fluctuation-renormalized Josephson coupling and the interplay between multiple energy scales. In principle, a quantitative agreement with specific experimental systems could be achieved by tuning the microscopic Josephson parameters (J_1 , J_2 , and α) and disorder strength (τ). However, a detailed fitting to individual experiments is beyond the scope of the present work, whose primary goal is to establish the general theoretical framework and the underlying physical mechanism.

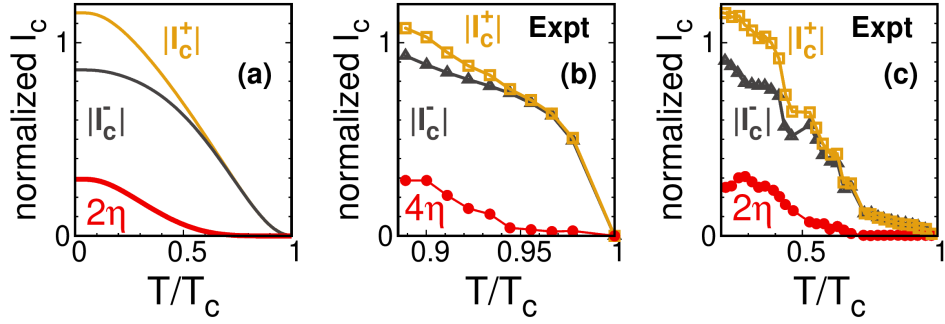


FIG. SI. (a) Reproduction of Fig. 3(b) in the main text, showing the theoretical temperature dependence of the forward and backward critical currents. (b) and (c) Experimental results extracted from Ref. [61] and Ref. [62], respectively, displaying the temperature evolution of $|I_c^+(T)|$ and $|I_c^-(T)|$. The qualitative merging of the two critical currents with increasing temperature is consistent with our theoretical prediction.

SV. Zero-point oscillations

Finally, we discuss the influence of zero-point fluctuations of the Josephson phase mode. Focusing on the zero-temperature limit, as shown in Fig. SII, increasing disorder (left panel) and reducing the Fermi velocity (right panel) both suppress the phase stiffness, leading to a reduction of the zero-temperature Josephson critical current $I_c(0)$ and the diode efficiency $\eta(0)$.

This behavior originates from the softening of the Josephson phase mode (at finite q) when the phase stiffness decreases. A weaker stiffness enlarges the available phase space of the collective-mode integration, thereby enhancing zero-point phase fluctuations. Through the Debye–Waller–type exponential renormalization factor, these enhanced quantum fluctuations suppress the effective Josephson coupling $\bar{J}_1(0)$ and $\bar{J}_2(0)$. As a consequence, both the zero-temperature critical current $I_c(0)$ and the diode efficiency $\eta(0)$ are reduced.

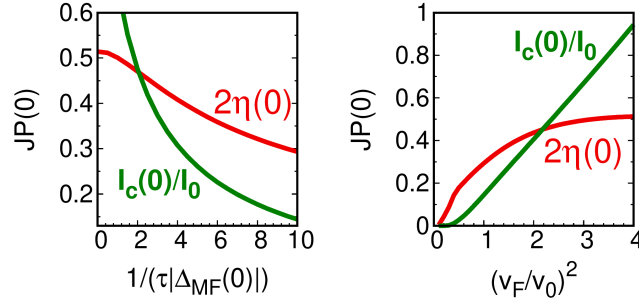


FIG. SII. Zero-temperature Josephson critical current $I_c(0)$ and diode efficiency $\eta(0)$ under varying phase stiffness conditions. Left panel: Increasing disorder at $v_F = v_0$. Right panel: Reducing the Fermi velocity at $\tau|\Delta_{MF}(0)| = 0.1$. Here, $v_0 = 10^5$ m/s and $I_0 = 60 \mu\text{A}/\mu\text{m}^2$.

This zero-point effect suggests the intrinsic quantum sensitivity of low-dimensional Josephson-diode systems. Importantly, because this suppression originates from quantum zero-point fluctuations rather than thermal effects, it represents a fundamental quantum limitation that cannot be circumvented by cooling. It indicates that enhancing phase stiffness (through improved material quality, reduced disorder, or optimized carrier density) is essential for robust device functionality and for maximizing nonreciprocal Josephson performance, particularly in low-dimensional systems.

-
- [1] J. Schrieffer, *Theory of Superconductivity* (W.A. Benjamin, 1964).
[2] M. E. Peskin, *An introduction to quantum field theory* (CRC press, 2018).
[3] B. Pal, A. Chakraborty, P. K. Sivakumar, M. Davydova, A. K. Gopi, A. K. Pandeya, J. A. Krieger, Y. Zhang, M. Date, S. Ju, N. Yuan, N. B. M. Schröter, L. Fu, and S. S. P. Parkin, Josephson diode effect from cooper pair momentum in a topological semimetal, *Nat. Phys.* **18**, 1228 (2022).
[4] P. A. Volkov, E. Lantagne-Hurtubise, T. Tummuru, S. Plugge, J. H. Pixley, and M. Franz, Josephson diode effects in twisted nodal superconductors, *Phys. Rev. B* **109**, 094518 (2024).

- [5] O. Can, T. Tummuru, R. P. Day, I. Elfimov, A. Damascelli, and M. Franz, High-temperature topological superconductivity in twisted double-layer copper oxides, *Nat. Phys.* **17**, 519 (2021).
- [6] Z. Sun, M. M. Fogler, D. N. Basov, and A. J. Millis, Collective modes and terahertz near-field response of superconductors, *Phys. Rev. Res.* **2**, 023413 (2020).
- [7] A. A. Abrikosov, L. P. Gorkov, and I. E. Dzyaloshinski, *Methods of quantum field theory in statistical physics* (Courier Corporation, 2012).
- [8] G. D. Mahan, *Many-particle physics* (Springer Science & Business Media, 2013).
- [9] G. Tkachov, Magnetoelectric andreev effect due to proximity-induced nonunitary triplet superconductivity in helical metals, *Phys. Rev. Lett.* **118**, 016802 (2017).
- [10] V. Ambegaokar and L. P. Kadanoff, Electromagnetic properties of superconductors, *Il Nuovo Cimento* **22**, 914 (1961).
- [11] F. Yang and M. W. Wu, Theory of coupled dual dynamics of macroscopic phase coherence and microscopic electronic fluids: Effect of dephasing on cuprate superconductivity, *Phys. Rev. B* **104**, 214510 (2021).
- [12] F. Yang and M. W. Wu, Gauge-invariant microscopic kinetic theory of superconductivity: Application to the optical response of Nambu-Goldstone and Higgs modes, *Phys. Rev. B* **100**, 104513 (2019).
- [13] F. Yang and M. W. Wu, Gauge-invariant microscopic kinetic theory of superconductivity in response to electromagnetic fields, *Phys. Rev. B* **98**, 094507 (2018).
- [14] A. J. Leggett, Number-phase fluctuations in two-band superconductors, *Prog. Theor. Phys.* **36**, 901 (1966).
- [15] P. Fulde and R. A. Ferrell, Superconductivity in a strong spin-exchange field, *Phys. Rev.* **135**, A550 (1964).
- [16] F. Yang and M. W. Wu, Fulde-Ferrell state in spin-orbit-coupled superconductor: Application to Dresselhaus SOC, *J. Low Temp. Phys.* **192**, 241 (2018).
- [17] F. Yang and M. W. Wu, Gapped superconductivity with all symmetries in insb (110) quantum wells in proximity to *s*-wave superconductor in fulde-ferrell-larkin-ovchinnikov phase or with a supercurrent, *Phys. Rev. B* **95**, 075304 (2017).
- [18] F. Yang and L. Chen, A tractable framework for phase transitions in phase-fluctuating disordered 2D superconductors: applications to bilayer MoS₂ and disordered InO_x thin films, arXiv:2511.13268 (2025).
- [19] F. Yang, G. Zhao, Y. Shi, and L. Chen, An efficient phase-transition framework for gate-tunable superconductivity in monolayer WTe₂, arXiv:2509.08332 (2025).
- [20] F. Yang, Y. Shi, and L.-Q. Chen, Preformed cooper pairing and the uncondensed normal-state component in phase-fluctuating cuprate superconductivity, arXiv:2509.21133 (2025).
- [21] F. Yang and M. W. Wu, Impurity scattering in superconductors revisited: Diagrammatic formulation of the supercurrent-supercurrent correlation and Higgs-mode damping, *Phys. Rev. B* **106**, 144509 (2022).
- [22] G. Eilenberger, Transformation of Gorkov's equation for type II superconductors into transport-like equations, *Z. Phys.* **214**, 195 (1968).
- [23] K. D. Usadel, Generalized diffusion equation for superconducting alloys, *Phys. Rev. Lett.* **25**, 507 (1970).
- [24] M. Silaev, Nonlinear electromagnetic response and Higgs-mode excitation in BCS superconductors with impurities, *Phys. Rev. B* **99**, 224511 (2019).
- [25] M. Tinkham, *Introduction to superconductivity*, Vol. 1 (Courier Corporation, 2004).
- [26] D. C. Mattis and J. Bardeen, Theory of the anomalous skin effect in normal and superconducting metals, *Phys. Rev.* **111**, 412 (1958).
- [27] F. Yang and M. W. Wu, Diamagnetic property and optical absorption of conventional superconductors with magnetic impurities in linear response, *Phys. Rev. B* **109**, 064508 (2024).
- [28] S. B. Nam, Theory of electromagnetic properties of superconducting and normal systems. i, *Phys. Rev.* **156**, 470 (1967).
- [29] T. R. Lemberger, I. Hetel, J. W. Knepper, and F. Y. Yang, Penetration depth study of very thin superconducting nb films, *Phys. Rev. B* **76**, 094515 (2007).
- [30] A. I. Gubin, K. S. Il'in, S. A. Vitusevich, M. Siegel, and N. Klein, Dependence of magnetic penetration depth on the thickness of superconducting nb thin films, *Phys. Rev. B* **72**, 064503 (2005).
- [31] C. Varmazis and M. Strongin, Inductive transition of niobium and tantalum in the 10-mhz range. i. zero-field superconducting penetration depth, *Phys. Rev. B* **10**, 1885 (1974).
- [32] G. E. Peabody and R. Meservey, Magnetic flux penetration into superconducting thin films, *Phys. Rev. B* **6**, 2579 (1972).
- [33] C. Kittel and C.-y. Fong, *Quantum theory of solids*, Vol. 5 (Wiley New York, 1963).
- [34] J. J. Sakurai and J. Napolitano, *Modern quantum mechanics* (Cambridge University Press, 2020).
- [35] L. D. Landau, E. M. Lifshitz, and L. P. Pitaevskii, *Statistical Physics, Part 1* (Pergamon, New York, 1980).
- [36] L. Benfatto, *The Berezinskii-Kosterlitz-Thouless Transition and its Application to Superconducting Systems* (2024).
- [37] Y. Nambu, Quasi-particles and gauge invariance in the theory of superconductivity, *Phys. Rev.* **117**, 648 (1960).
- [38] J. Goldstone, Field theories with "superconductor" solutions, *Il Nuovo Cimento* **19**, 154 (1961).
- [39] J. Goldstone, A. Salam, and S. Weinberg, Broken symmetries, *Phys. Rev.* **127**, 965 (1962).
- [40] Y. Nambu, Nobel lecture: Spontaneous symmetry breaking in particle physics: A case of cross fertilization, *Rev. Mod. Phys.* **81**, 1015 (2009).
- [41] P. W. Anderson, Plasmons, gauge invariance, and mass, *Phys. Rev.* **130**, 439 (1963).
- [42] P. B. Littlewood and C. M. Varma, Gauge-invariant theory of the dynamical interaction of charge density waves and superconductivity, *Phys. Rev. Lett.* **47**, 811 (1981).
- [43] S. Fischer, M. Hecker, M. Hoyer, and J. Schmalian, Short-distance breakdown of the Higgs mechanism and the robustness of the BCS theory for charged superconductors, *Phys. Rev. B* **97**, 054510 (2018).
- [44] L. Benfatto, A. Toschi, S. Caprara, and C. Castellani, Phase fluctuations in superconductors: From galilean invariant to quantum XY models, *Phys. Rev. B* **64**, 140506 (2001).
- [45] L. Benfatto, A. Toschi, and S. Caprara, Low-energy phase-only action in a superconductor: A comparison with the XY model, *Phys. Rev. B* **69**, 184510 (2004).
- [46] i. c. v. Kos, A. J. Millis, and A. I. Larkin, Gaussian fluctuation corrections to the BCS mean-field gap amplitude at zero temperature, *Phys.*

Rev. B **70**, 214531 (2004).

- [47] P. W. Anderson, Theory of dirty superconductors, *J. Phys. Chem. Solids* **11**, 26 (1959).
- [48] H. Suhl and B. T. Matthias, Impurity scattering in superconductors, *Phys. Rev.* **114**, 977 (1959).
- [49] S. Skalski, O. Betbeder-Matibet, and P. R. Weiss, Properties of superconducting alloys containing paramagnetic impurities, *Phys. Rev.* **136**, A1500 (1964).
- [50] L. Andersen, A. Ramires, Z. Wang, T. Lorenz, and Y. Ando, Generalized Anderson's theorem for superconductors derived from topological insulators, *Sci. Adv.* **6**, eaay6502 (2020).
- [51] T. Song, Y. Jia, G. Yu, Y. Tang, P. Wang, R. Singha, X. Gui, A. J. Uzan-Narovlansky, M. Onyszczak, K. Watanabe, T. Taniguchi, R. J. Cava, L. M. Schoop, N. P. Ong, and S. Wu, Unconventional superconducting quantum criticality in monolayer wTe_2 , *Nat. Phys.* **20**, 269 (2024).
- [52] T. Song, Y. Jia, G. Yu, Y. Tang, A. J. Uzan, Z. J. Zheng, H. Guan, M. Onyszczak, R. Singha, X. Gui, K. Watanabe, T. Taniguchi, R. J. Cava, L. M. Schoop, N. P. Ong, and S. Wu, Unconventional superconducting phase diagram of monolayer wTe_2 , *Phys. Rev. Res.* **7**, 013224 (2025).
- [53] E. Sajadi, T. Palomaki, Z. Fei, W. Zhao, P. Bement, C. Olsen, S. Luescher, X. Xu, J. A. Folk, and D. H. Cobden, Gate-induced superconductivity in a monolayer topological insulator, *Science* **362**, 922 (2018).
- [54] V. Fatemi, S. Wu, Y. Cao, L. Bretheau, Q. D. Gibson, K. Watanabe, T. Taniguchi, R. J. Cava, and P. Jarillo-Herrero, Electrically tunable low-density superconductivity in a monolayer topological insulator, *Science* **362**, 926 (2018).
- [55] O. Zheliuk, J. M. Lu, Q. H. Chen, A. A. El Yumin, S. Golightly, and J. T. Ye, Josephson coupled ising pairing induced in suspended mos_2 bilayers by double-side ionic gating, *Nat. Nanotechnol.* **14**, 1123 (2019).
- [56] T. Charpentier, D. Perconte, S. Léger, K. R. Amin, F. Blondelle, F. Gay, O. Buisson, L. Ioffe, A. Khvalyuk, I. Poboiko, M. Feigel'man, N. Roch, and B. Sacépé, First-order quantum breakdown of superconductivity in an amorphous superconductor, *Nat. Phys.* **21**, 104 (2025).
- [57] J. B. Curtis, N. Maksimovic, N. R. Poniatowski, A. Yacoby, B. Halperin, P. Narang, and E. Demler, Probing the Berezinskii-Kosterlitz-Thouless vortex unbinding transition in two-dimensional superconductors using local noise magnetometry, *Phys. Rev. B* **110**, 144518 (2024).
- [58] L. Benfatto, C. Castellani, and T. Giamarchi, Broadening of the Berezinskii-Kosterlitz-Thouless superconducting transition by inhomogeneity and finite-size effects, *Phys. Rev. B* **80**, 214506 (2009).
- [59] L. Benfatto, C. Castellani, and T. Giamarchi, Doping dependence of the vortex-core energy in bilayer films of cuprates, *Phys. Rev. B* **77**, 100506 (2008).
- [60] J. Yong, T. R. Lemberger, L. Benfatto, K. Ilin, and M. Siegel, Robustness of the Berezinskii-Kosterlitz-Thouless transition in ultrathin NbN films near the superconductor-insulator transition, *Phys. Rev. B* **87**, 184505 (2013).
- [61] Z. Wei, Y. Qiao, Y.-Y. Lyu, D. Wang, T. Li, L. R. Cadornim, P. Zhang, W.-C. Yue, D. Li, Z. Song, *et al.*, Scalable high-temperature superconducting diodes in intrinsic josephson junctions, *arXiv:2508.06083* (2025).
- [62] M. S. Anwar, T. Nakamura, R. Ishiguro, S. Arif, J. W. A. Robinson, S. Yonezawa, M. Sigrist, and Y. Maeno, Spontaneous superconducting diode effect in non-magnetic Nb/Ru/Sr₂RuO₄ topological junctions, *Commun. Phys.* **6**, 290 (2023).